Transferring functional chromosomes between intergeneric yeast generates monochromosomal hybrids with improved phenotypes and widespread transcriptional responses

Authors

Yilin Lyu[1,2], Kunfeng Song[1,2], Jungang Zhou[1,2], Hao Chen[3], Xueying C. Li[4,*], Yao Yu[1,2,*]and Hong Lu[1,2]

Affiliations

[1] School of Life Sciences, State Key Laboratory of Genetics and Development of Complex Phenotypes, Fudan University, Shanghai, China.

[2] Shanghai Engineering Research Center of Industrial Microorganisms, Shanghai, China.

[3] Personal Oncology Inc., Nanjing, Jiangsu Province, China.

[4] Ministry of Education Key Laboratory for Biodiversity Science and Ecological Engineering, College of Life Sciences, Beijing Normal University, Beijing, China.

[*] Corresponding authors. Emails: yaoyu@fudan.edu.cn; lixueying@bnu.edu.cn.

Abstract

Interspecific hybrids can exhibit phenotypes that surpass those of their parents, known as heterosis, which is often of interest for industrial applications and evolutionary genetics research. However, constructing hybrids between distantly related species, such as intergeneric yeasts, presents technical challenges. In this study, we established a method to transfer individual chromosomes from *Saccharomyces cerevisiae* (Sc) into *Kluyveromyces marxianus* (Km), an emerging model for bioproduction. The Sc chromosome of interest was circularized, genetically modified to carry Km centromeres and replication origins, and transformed into Km via protoplast transformation. With this method, we generated monochromosomal hybrids with eight Km chromosomes and Sc chromosome I or III. The Sc chromosomes exhibited normal replication, segregation, and active transcription in the hybrids. The hybrids displayed heterosis in flocculation and salt tolerance due to the overexpression of *FLO9* and *SPS22* on transferred Sc chromosome, respectively. Transcriptomic analysis revealed that both *cis*- and *trans*-regulatory changes contributed to the divergence of gene expression between the two species, with the *cis* and *trans* effects

often acting in a compensatory manner. Our strategy has potential applications in optimizing cell factories, constructing synthetic genomes, and advancing evolutionary research.

Teaser

A yeast hybrid containing an alien chromosome transferred from a distantly related species exhibits improved phenotypes.

MAIN TEXT

Introduction

The transfer of genetic materials between species is one of the major driving forces for speciation and environmental adaptation [1,2]. Chromosomes, which carry packs of genes, can introduce abundant genetic variation and contribute to evolution of adaptive traits when transferred between species. For example, horizontal transfer of plastid chromosomes between tobacco plants (*Nicotiana*) aided chloroplast capture [3]. Horizontal transfer of chromosomes between *Fusarium* species, a group of filamentous fungi, led to new pathogenic lineages [4]. Furthermore, hybridization is by nature a process of interspecific chromosome transfers. With the combined genetic materials, hybrids often exhibit enhanced phenotypes, known as heterosis or hybrid vigor. For example, hybridization between the top-fermenting yeast *Saccharomyces cerevisiae* and the cold-tolerant *S. eubayanus* gave rise to one of the most important lager-brewing species, *S. pastorianus* [5]. Similarly, triticale, a hybrid of rye (*Secale cereale*) and wheat (*Triticum aestivum L.*), exhibited improved yield in marginal environments [6]. Therefore, introduction of genetic materials from a distantly related species may hold great potential for phenotypic improvement in the fields of crop breeding and industrial applications.

Understanding the phenotypic and molecular consequences of interspecific hybridization may also address many important questions in genome evolution. For example, what are the molecular bases for heterosis [7]? From the perspective of gene regulation, can distantly related genomes regulate each other [8]? Is there an upper limit for evolutionary divergence such that two genomes with a divergence level above this threshold cannot regulate each other anymore? Is evolution of gene expression predominantly driven by *cis*- or *trans*-regulatory changes [9]? Many previous studies have addressed these questions with natural or synthetic hybrids [10–17], including important conclusions that sequence divergence in *cis*-regulatory elements such as promoters and enhancers, as well as compensatory *trans*-acting changes, became increasingly important for evolution of gene expression as

evolutionary distance increases [16]. However, many of these questions remain open for distantly related species where natural hybrids are not available.

In this study, we explore the phenotypic and molecular consequences of hybridization between *Kluyveromyces marxianus* and *S. cerevisiae*, by synthetically constructing monochromosomal hybrids between the two distantly related species. *K. marxianus* is a yeast species that belongs to the *Saccharomycetaceae* family but only distantly related to *S. cerevisiae* (**Fig. 1A**). It has been previously argued that it may serve as an emerging model for bioproduction, including heterologous proteins, bioethanol and bulk chemicals [18,19]. It has a number of traits different from *S. cerevisiae*, including a high growth rate, thermotolerance, and the ability to assimilate a wide variety of sugars [20–22]. On the other hand, *S. cerevisiae* is more tolerant to ethanol than *K. marxianus* [19]. It is widely used in industrial fermentation and has arguably the best studied genome among eukaryotes [23]. Mixing the genetic materials between the two species is expected to provide novel phenotypes for industrial development, as well as to understand their evolution.

Stable allodiploid hybrids between *K. marxianus* and *S. cerevisiae* haven't been made available, although partial integration of *S. cerevisiae* genome fragments into *K. marxianus* has been achieved by protoplast fusion [24,25]. In order to introduce *S. cerevisiae* genetic materials in a systematic, controllable manner, we developed a genetic-engineering strategy to artificially transfer chromosomes between the two species. Artificial chromosome transfer was first established in 1977, when murine chromosomes were transferred into human cells via microcells [26]. To date, artificial transfer of functional chromosomes has primarily been achieved between closely related species (dashed lines, **Fig. 1B**), including transfers of human chromosome 21 into mouse and chicken cells [27–29], and between bacteria species *Mycoplasma mycoides* and *M. capricolum* [30]. *S. cerevisiae* (Sc) and *K. marxianus* (Km) diverged 114 million years ago [31], significantly exceeding the evolutionary distance between the species that have been shown capable of natural or artificial chromosome transfers (**Fig. 1B**). Previous efforts of protoplast fusion showed that Sc genomes are often unstable after the fusion with Km [25]. One possible explanation is the incompatibility of replicating elements such as centromere (*CEN*) and autonomously replicating sequence (*ARS*), as previously shown in hybrid incompatibility studies [32,33]. In this study, we engineered the Sc chromosome to resolve potential incompatibilities, including circularization of the chromosome and insertion of *ARS* and *CEN* from the host species [34]. The engineered Sc chromosome was transformed into Km, creating a monochromosomal hybrid. Through phenotypic and gene expression analysis, we showed that functional chromosome transfer between distantly

related species can produce beneficial phenotypes associated with overexpression of genes from the Sc chromosome. The transferred chromosomes triggered widespread transcriptional responses in the transferred and host genomes, suggesting cross-species regulation. Finally, we found that divergence of gene expression of the two species is often contributed by compensating *cis*- and *trans*-regulatory changes, providing new evidence for regulatory evolution across a long evolutionary timescale. Our strategy has potential applications in optimizing microbial cell factories and advancing evolutionary studies.

Results

Compatibility of ARS and CEN between Sc and Km

It is critical to ensure proper replication and segregation of the heterologous chromosome upon chromosome transfer. Therefore, we started by investigating the compatibility of *ARS* and *CEN* between Sc and Km. We examined transformation success and stability of plasmids carrying different combinations of *KmARS1*, *KmCEN5*, *ScARSH4* and *ScCEN6*. We found that *KmARS1* and *KmCEN5* was respectively essential for successful transformation (**Fig. 1C**, left**)** and plasmid maintenance in Km (**Fig. 1D**, left). Neither could be replaced by their Sc counterparts, *ScARSH4* and *ScCEN6*, suggesting incompatibility. Plasmids carrying *KmCEN5+KmARS1* produced transformants in Sc (**Fig. 1C**, right), but with poor stability (**Fig. 1D**, right), suggesting that *KmARS1* but not *KmCEN5* can function in Sc. Similar results were obtained using combinations of *KmARS18*, *KmCEN3*, *ScARS1* and *ScCEN4* (**Fig. S1**). The observed incompatibility could explain the rapid loss of Sc chromosomes in previous protoplast fusion between Km and Sc [25]. Finally, the plasmid containing both *ARS*s and *CEN*s from Sc and Km, known as double *CEN/ARS* plasmid, could replicate and segregate stably in both Km and Sc (**Fig. 1C**, left). Therefore, the issue of Sc chromosomal instability in Km may be resolved by engineering *KmCEN* and *KmARS* into Sc chromosomes.

Using double *CEN/ARS* plasmids carrying different antibiotic markers, we examined the mating rate between Km and Sc. We transformed haploid Km and Sc cells with plasmids carrying the kan^R or hyg^R marker, mixed them in different combinations (see **Methods**) and selected for zygotes on double antibiotic medium (**Fig. 1E**). The results showed that the mating efficiency between Km *MAT***a** and *MAT*α cells, as well as between Sc *MAT***a** and *MAT*α cells, was around 16%. However, mixing 1.6×10^7 Km cells with 1.6×10^6 Sc cells, regardless of their mating types, failed to yield any zygotes, based on both double selection (**Fig. 1E**) and microscopic observation (**Fig. S2**). These results demonstrated a prezygotic

reproductive barrier between the two species, which urges a synthetic method for generating Km-Sc hybrids.

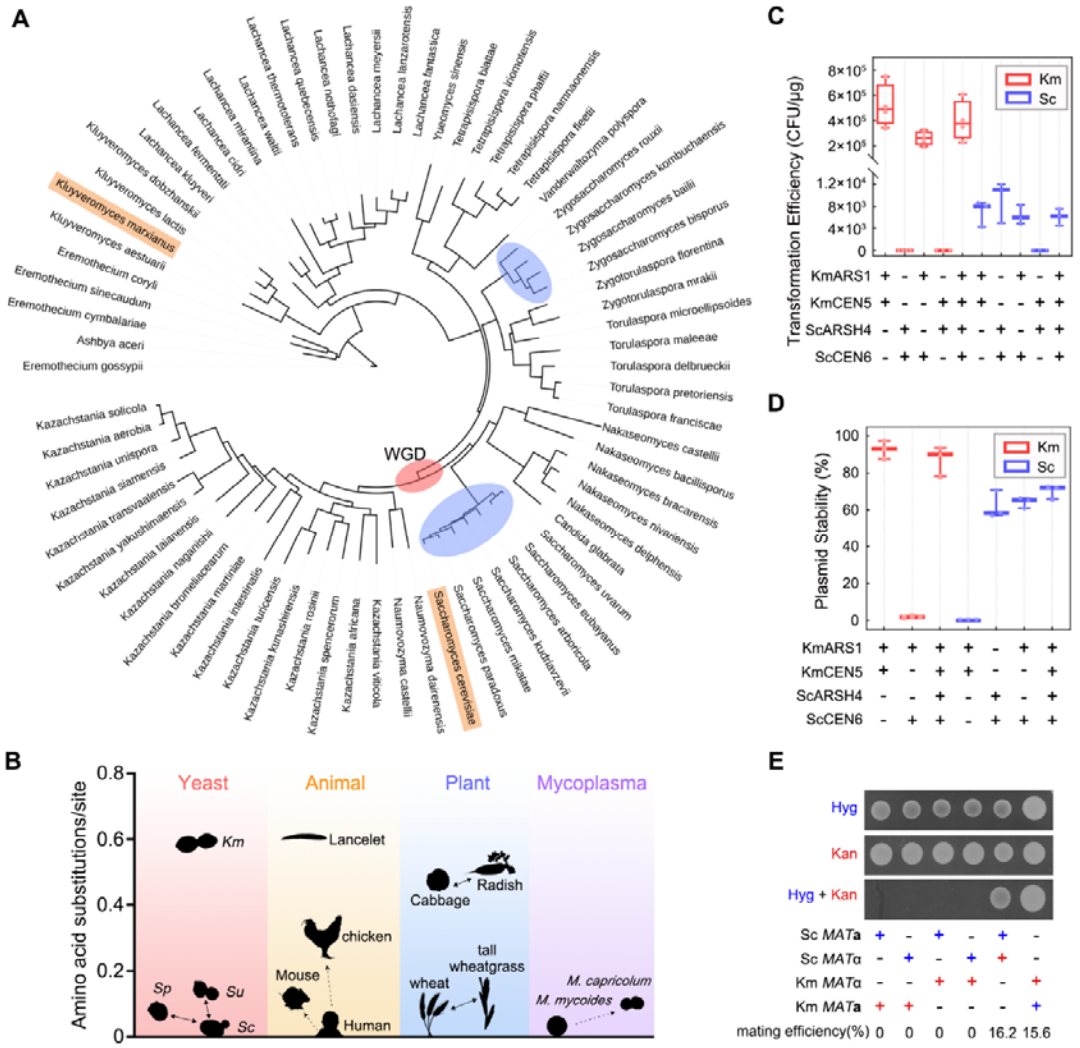

Fig. 1. Functionality of ARS and CEN in Sc and Km. (A) Phylogenetic tree of the *Saccharomycetaceae* family based on 71 selected species. Blue ellipses show species capable of interspecific hybridization, while red ellipse marks the event of whole-genome duplication. Sc and Km are highlighted in orange. The tree was constructed with iqtree2 [35] with concatenated coding sequences of 2,408 orthologous groups [31]. **(B)** The evolutionary distance between Km and Sc, compared to species in other taxa that are capable of interspecific hybridization (solid lines) or tolerant to chromosomal transfer (dashed lines). Data of amino acid substitutions per site were generated by Orthofinder2 [36]. Sp, *Saccharomyces paradoxus*. Su, *S. uvarum*. **(C, D)** Transformation efficiency **(C)** and stability **(D)** of plasmids containing different combinations of *ARS* and *CEN* alleles in the two species (blue for Sc, red for Km). Stability refers to the percentage of cells containing the plasmid after being grown in non-selective YPD medium for 24 h. Lines in the boxplots and whiskers show the median, maximum and minimum values. **(E)** Mating assay between Km and Sc. Haploid Km or Sc cells containing a *kanR* (red cross) or *hygR* (blue cross) plasmid were mixed and spotted onto a medium containing hygromycin (Hyg), kanamycin (Kan), or both. Mating efficiency was

quantified by counting double-resistant colonies (see **Methods**), represented by the mean of three replicate experiments.

Engineering and transferring Sc chromosomes into Km

We selected the smallest Sc chromosome, chrI (252 kb, 85 genes based W303 annotation), and the third smallest chromosome, chrIII (341 kb, 156 genes), for proof-of-principle experiments of Sc-Km chromosomal transfer. The experimental pipeline is shown in **Fig. 2A**. First, we circularized the chromosomes of interest to avoid potential incompatibility of telomeres. Sc telomeres (TELs) are composed of TG_{1-3} repeat sequences, while Km TELs consist of a long repeat motif (25 nt) [37]. We removed the TELs from chrI and chrIII, respectively, and joined the ends with *KmURA3* with CRISPR/Cas9 [38]. To avoid homologous recombination at the telomeres, the telomere-associated long repetitive sequence on chr1 was deleted during circularization [38]. Next, to ensure stable maintenance of Sc chromosomes in Km, we inserted *KmCEN5* /*ARS1* adjacent to the native *CEN*s on chrI and chrIII. Given that chrI and chrIII contain 5 and 12 *ARS*s, respectively [39], we placed another copy of *KmARS1* close to a native *ScARS*, which was about ∼100 kb away from the *KmCEN5* /*ARS1* in the circular chromosomes (see **Methods** for details). The engineered circular chrI and chrIII were named R1 and R3, respectively. Sc cells with R1 ("Sc-R1") or R3 ("Sc-R3") showed no fitness defect under normal culture conditions as well as in the presence of microtubule-depolymerizing and DNA-damaging agents (**Fig. S3**), indicating that the introduction of *KmARS1* and *KmCEN5* did not affect chromosome replication in Sc. The circularization was confirmed by pulsed-field gel electrophoresis (PFGE), which showed an absence of linear chrI or chrIII in the gel (**Fig. 2B**). Following a protocol developed by Noskov et al. [40], we extracted and column-purified R1 and R3, with the undesired linear chromosomes removed by exonuclease. Finally, the purified R1 and R3 were separately transformed into Km using protoplast transformation [41], yielding four R1 transformants (*Kluyveromyces*-*Saccharomyces*-R1, "KS-R1" hereafter) and one R3 transformant ("KS-R3"). The low number of transformants indicates a need for further optimization of the transformation protocol, especially for transferring larger chromosomes.

We next examined the integrity of the transferred chromosomes. All four KS-R1 transformants retained six Sc-specific markers located on R1 (**Fig. 2C**, see **Table S1** for marker positions), indicating successful transfer of R1. The transfer was further confirmed by restriction digest (**Fig. 2E**) and whole genome sequencing, which found no mutations in the transferred R1. In PCR analysis of KS-R3, marker 7 was absent (**Fig. 2D**). PFGE analysis

showed that the size of linearized R3 was smaller than the expected 340 kb (**Fig. 2E**). Genome sequencing revealed a 29 kb deletion between two direct repeats of putative Ty elements in R3 (**Figs. 2F & S4**). The deletion was potentially due to homologous recombination between Ty elements, the rate of which has been shown to significantly increase in circular plasmids during transformation [42]. The deleted region contained 13 genes (*MAK32*, *PET18*, *MAK31*, *HTL1*, *HSP30*, *YCR022C*, *YCR023C*, *SLM5*, *YCR024C-B*, *PMP1*, *YCR025C*, *NPP1*, *RHB1*). We introduced the deleted region, in six individual segments via plasmids, into Km cells (**Fig. S4**). None of the segments affected growth (**Fig. S4**), excluding the possibility that the loss of the 29 kb region was an adaptive response to overcome incompatibility.

We next evaluated the Km genome integrity after transformation. The PFGE patterns of Km chromosomes in KS-R1 and KS-R3 were consistent with the Km parent (**Fig. S5**). Genome sequencing revealed 33 mutations in 11 ORFs, as well as 82 SNPs and indels in intergenic sequences in Km chromosomes in KS-R1 (**Table S2**). KS- R3 contained 4 mutations in 4 ORFs, and 47 SNPs and indels in intergenic sequences (**Table S2**). These mutations might have been induced during the protoplast transformation. Overall, the transfer of R1 or R3 into Km did not result in fusions, translocations, or other large-scale rearrangements in the Km chromosomes, thus creating a monochromosomal hybrid containing eight Km chromosomes and one Sc chromosome.

Subsequently, we examined the hybrids for any fitness defects. In rich medium (YPD), the growth curves of KS-R1 and KS-R3 were indistinguishable from Km-V, the parental Km strain with a void vector (**Fig. 2G**). Under non-selective conditions, R1 and R3 were highly stable in the hybrids. The loss rate per generation for R1 and R3 in YPD was 0.11% and 0.84%, respectively (**Fig. 2H**), a level comparable to that of circular YACs in Km [43]. Furthermore, KS-R1 and KS-R3 exhibited robust growth in the presence of the microtubule-depolymerizing agents benomyl (BML) and thiabendazole (TBZ), DNA replication inhibitor hydroxyurea (HU), DNA-damaging agents methyl methane sulfonate (MMS) and camptothecin (CPT) [44], or protein synthesis inhibitor cycloheximide (CHX) (**Fig. 2I**). Taken together, the introduction of R1 and R3 did not affect growth, chromosome segregation, DNA replication, or protein synthesis of the hybrids in rich medium. The Km cells were tolerant to the transplantation of Sc chromosomes, reflecting cellular plasticity.

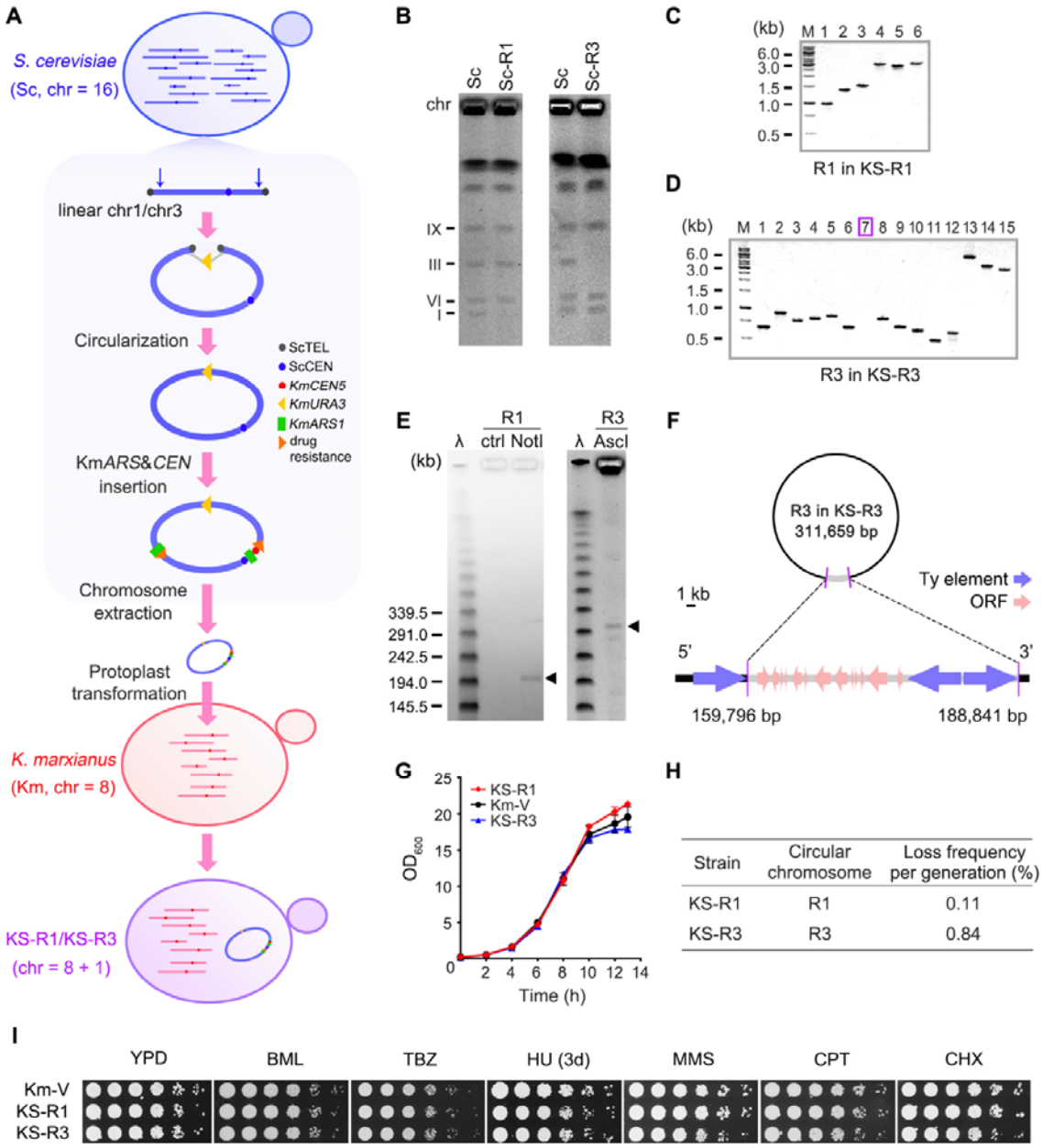

Fig. 2. Engineering and Transferring Sc Chromosomes into Km. (A) Experimental pipeline for transferring Sc chromosomes into Km. **(B)** PFGE of chromosomal extracts from Sc-R1, Sc-R3 and the parental Sc strain. **(C, D)** PCR of markers in the circular chromosomes in KS-R1 **(C,** represented by one transformant**)** and KS-R3 **(D)**. Purple box labels the missing marker, #7, in KS-R3. See **Table S1** for marker positions. **(E)** PFGE of R1 and R3 (arrows) in the hybrids, linearized with NotI and AscI respectively. Ctrl: non-digested KS-R1 chromosomal extracts. λ: Lambda PFG Ladder. **(F)** Illustration of the 29 kb deletion in R3 of KS-R3. Coordinates are based on a manually curated R1 sequence (**Table S1**). **(G)** Growth curves of KS-R1, KS-R3, and Km-V in YPD. The values represent mean ± SD (n=3). **(H)** Stability of circular chromosomes in hybrids. The values represent the mean (n=3). **(I)** Spot assay of KS-R1 and KS-R3 in the presence of benomyl (BML), thiabendazole (TBZ), hydroxyurea (HU), methyl methane sulfonate (MMS), camptothecin (CPT) or cycloheximide (CHX). Unless otherwise indicated, the plates were incubated at 30 degrees for 1 day.

Hybrids exhibit heterosis due to interactions between Km-encoded *trans*-factors and Sc *cis*-regulatory sequences

We next investigated if the transferred chromosomes conferred novel phenotypes. We treated the hybrids and their parents with twenty environmental conditions and semi-quantified their relative growth on solid media, using YPD growth as a reference (**Figs. 3A & S6**). The monochromosomal hybrids KS-R1 and KS-R3 exhibited comparable growth to Km-V under 19 and 15 conditions, respectively (**Fig. 3A**), suggesting that the small number of genes in R1 and R3 did not trigger a widespread metabolic reprogramming in Km. Under a few conditions, R1 and R3 caused growth defects, suggesting potential incompatibility. For instance, KS-R1 exhibited increased sensitivity to 42 □ and KS-R3 exhibited increased sensitivity to tunicamycin (TM) (**Fig. 3A-B**). The defective growth phenotypes were not shared by the two hybrids, indicating that the defects were caused by dominant effects of genes on R1 or R3, rather than a general effect caused by chromosomal transfers. Additionally, we ruled out the possibility that the mutations in the Km genome caused the phenotypes, because the strains no longer exhibited the phenotypes after losing the Sc chromosomes in non-selective medium (**Fig. S7**).

Interestingly, the chromosomal transfer resulted in heterosis. KS-R3 exhibited enhanced tolerance to high concentration of sodium chloride (NaCl) compared to its parents (**Fig. 3C**). The high-salt condition is a common stress in industrial processes. Therefore, increased tolerance to NaCl is a beneficial phenotype for industrial production [45]. We next investigated the molecular mechanisms by which R3 increased NaCl tolerance in the hybrid. Among the genes carried by R3, *ScSPS22* is involved in *β*-glucan synthesis and related to cell wall function [46]. In a previously published genome-wide screen, overexpressing *ScSPS22* reduced NaCl tolerance [47]. We thus tested if *ScSPS22* contributed to the enhanced NaCl tolerance of the hybrid. *ScSPS22*, along with its 1000 bp upstream sequence (promoter), was introduced into Km via a centromeric plasmid. We found that, in contrast to its role in Sc, *ScSPS22* increased NaCl tolerance of Km to the same level as KS-R3 (**Fig. 3C**, upper panel). Expressing the Km ortholog of *ScSPS22*, *KmSPS22* (*FIM1_814*), did not have an obvious effect (**Fig. 3C**, upper panel). This result indicates that *ScSPS22* is the causal gene for the increased NaCl tolerance in KS-R3. Additionally, overexpressing *ScSPS22* in Sc with centromeric or 2-micron plasmids reduced NaCl tolerance (**Fig. 3C**, lower panel), consistent with the previous report.

In order to understand the contribution of *cis*-regulatory and coding sequences (CDS) to the phenotypic effect of *ScSPS22*, we constructed a chimeric allele consisting of the promoter of *KmSPS22* and the CDS of *ScSPS22*, namely *Pkm-ScSPS22*. There was no substantial difference between *Pkm-ScSPS22* and *KmSPS22* when expressed with a centromeric plasmid (**Fig. 3C,** upper panel), suggesting a lack of functional divergence in the CDS. On the contrary, *Pkm-ScSPS22* conferred a much lower level of NaCl tolerance than *ScSPS22* driven by its endogenous promoter, indicating that the Sc promoter was causal for the increase in NaCl tolerance.

The different phenotypic effects of Sc and Km promoters suggest potential divergence in gene expression. Therefore, we analyzed the transcription level of *ScSPS22* and *KmSPS22* in the hybrid and parents by qPCR (**Fig. 3D**). The relative mRNA level of *ScSPS22* in KS-R3 was respectively 53 and 80 times higher than those in Sc-R3 with and without NaCl (**Fig. 3D**, right panel), suggesting that (1) a significant difference in *trans*-acting regulators for *ScSPS22* between Sc and KS-R3; and (2) the up-regulation of *ScSPS22* in KS-R3 is constitutive. The relative mRNA level of *KmSPS22* did not significantly differ between KS-R3 and Km-V (**Fig. 3D**, left panel), indicating little difference in the *trans*-acting factors for *KmSPS22* between Km and KS-R3.

When transformed into Km on a centromeric plasmid, the *ScSPS22* allele was expressed at the same level as *ScSPS22* in KS-R3 ($p > 0.05$ for both YPD and NaCl conditions, Student's t-test, **Fig. 3D**), suggesting that the promoter sequence of *ScSPS22* was causal for its up-regulation in KS-R3. The chimeric allele *Pkm-ScSPS22* drove lower expression than *ScSPS22* in Km, consistent with *cis*-regulatory divergence. In Sc-R3 background, expressing *ScSPS22* with centromeric or high-copy 2μ plasmids increased its relative mRNA level, but failed to match the level of *ScSPS22* in KS-R3, suggesting that the upregulation of *ScSPS22* in KS-R3 resulted from induction or derepression by Km-specific *trans*-acting factors, rather than increased gene copy number. Taken together, the phenotypic and expression analysis showed that the heterosis in NaCl resistance was caused by specific interactions between Km-encoded *trans*-acting regulators and the Sc promoter of *SPS22*.

Although KS-R1 did not show any significant heterosis in the twenty conditions shown in **Fig. 3A**, we found that it exhibited a flocculation phenotype surpassing that of the parental Km-V and Sc-R1 (**Fig. 3E&F**). The flocculation phenotype disappeared after the loss of R1, indicating that R1 is responsible for the enhanced flocculation (**Fig. S8**). Flocculation facilitates cell sedimentation, reducing separation costs in high-density fermentation [48]. The *FLO* family genes control flocculation [49], among which *ScFLO9* is

present on R1. Introducing *ScFLO9* with its 1000 bp upstream sequence into Km via a centromeric plasmid enhanced flocculation to the same level as KS-R1 (**Fig. 3E&F**). This result suggests that *ScFLO9* is responsible for the increased flocculation phenotype in KS-R1. Overexpressing *ScFLO9* with a centromeric or 2μ plasmid in Sc slightly enhanced flocculation (**Fig. 3E&F**), consistent with its known role in Sc but suggesting its effect is background dependent.

We similarly analyzed the expression level of *FLO9* to understand the molecular mechanisms of the heterosis phenotype. qPCR showed that the relative mRNA level of *ScFLO9* in KS-R1 was 64.5 times higher than in Sc-R1 (**Fig. 3G**), again suggesting a significant change in the *trans*-regulatory environment. The high expression in KS-R1 was recapitulated by *ScFLO9* expression from a centromeric plasmid in Km (light pink bars in **Fig. 3G**, $p > 0.05$, Student's t-test). The expression level of *KmFLO5* (*FIM1_6*), the *ScFLO9* ortholog, was not increased in KS-R1, consistent with a lack of change in *trans* environment for Km genes (**Fig. 3G**, left panel). Overexpressing *ScFLO9* in Sc-R1 with centromeric and 2μ plasmids led to an increase in the mRNA level of *ScFLO9* expression (purple bars in **Fig. 3G**), with the higher level of $ScFLO9_{2\mu}$ correlating with faster flocculation (**Fig. 3F**). Taken together, the enhanced flocculation of KS-R1 was associated with *ScFLO9* being exposed to an alien *trans*-regulatory environment encoded by the Km genome. In both cases of *SPS22* and *FLO9*, the genetic combinations between Km-encoded *trans*-factors and Sc-encoded *cis*-factors would never be found in nature due to reproductive isolation, demonstrating the power of cross-species synthetic biology.

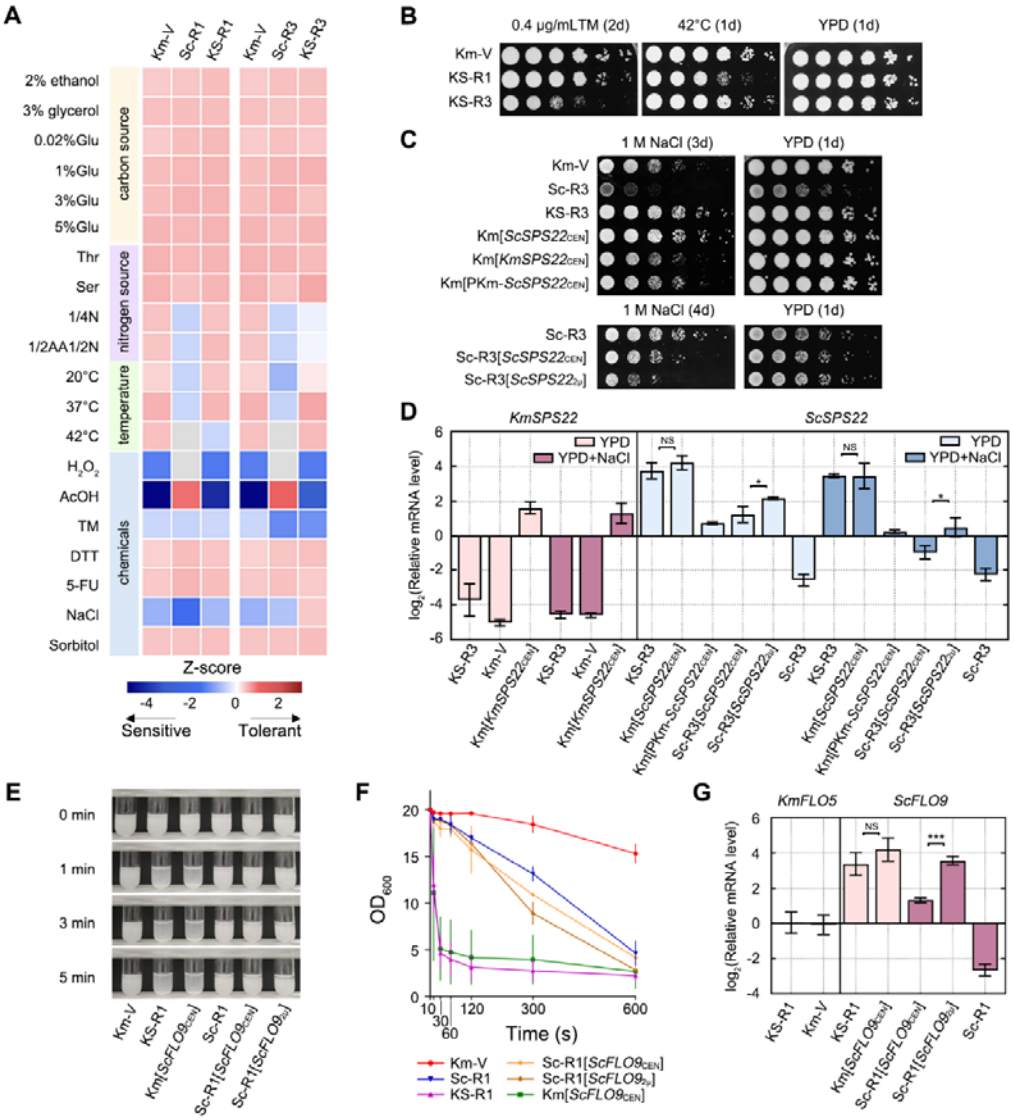

Fig. 3. Hybrids exhibit heterosis. (A) Growth phenotypes of hybrids and their parental strains under various conditions. Relative growth was semi-quantified through greyscale scanning of images from spot assays and normalized to YPD growth. Original images are provided in **Fig. S6**. The heatmap shows Z-scores of $\log_2$-transformed data. Grey denotes conditions where the strain could not grow. Glu, glucose; 1/4 N, one-quarter ammonium sulfate; 1/2 AA, half amino acids; 1/2 N, half ammonium sulfate; TM, tunicamycin; 5-FU, 5-fluorouracil. **(B)** Growth defects under tunicamycin or 42°C treatment associated with the transferred Sc chromosomes. **(C)** Improved NaCl tolerance associated with the promoter sequence of *ScSPS22*. *ScSPS22*, *KmSPS22* and *PKm-ScSPS22* alleles were expressed with a centromeric plasmid (indicated by the subscript CEN) or a 2μ plasmid ($ScSPS22_{2\mu}$) in either Km (upper panel) or Sc-R3 (lower panel). Serial dilutions were performed at 1:5 for all spot assays in this study. **(D)** Relative mRNA levels of *ScSPS22* and *KmSPS22* measured by qPCR. mRNA levels in the hybrid and Km cells were normalized to the average level of three housekeeping genes, *KmSWC4*, *KmTRK1*, and *KmMPE1*. mRNA levels of *ScSPS22* in Sc were normalized to the average level of *ScSWC4*, *ScTRK1*, and *ScMPE1*. The values represent the mean ± SD (n=3). **(E, F)** Enhanced flocculation in KS-R1 associated with *ScFLO9*. *ScFLO9* was expressed with either a centromeric plasmid ($ScFLO9_{CEN}$) or a 2μ

plasmid (*ScFLO9*$_{2\mu}$) in Km or Sc-R1. The strains were cultured overnight in SD-Ura or SD-Leu (see **Methods**) to an OD_{600} of 20. The cultures were vortexed vigorously and left still, before being imaged **(E)** and examined for the OD_{600} of the supernatant **(F)** at designated timepoints. The values in **(F)** represent the mean ± SD (n=3). **(G)** Relative expression levels of *ScFLO9* and *KmFLO5* measured by qPCR and normalized as described above. The values represent the mean ± SD (n=3). *, $p<0.05$; ***, $p<0.001$. NS, not significant. P-values were based on t-tests.

Pervasive transcriptional responses triggered by chromosomal transfer

The experiments with *ScSPS22* and *ScFLO9* revealed significant changes in Sc gene expression after being transferred to Km. To determine if this is a general pattern, we analyzed transcriptomes of the hybrids (KS) and parental strains in YPD and under two stress conditions, 1 μg/mL tunicamycin (TM) and 1 M NaCl. The genes on R1 and on R3 were actively transcribed in the hybrids under the three conditions (read counts >5) (**Supplementary Data File 2**). However, their expression in hybrids poorly correlated with that in Sc, with an average correlation coefficient (R^2) of 0.38 for R1 genes and 0.32 for R3 genes (**Fig. 4A**). This correlation was substantially lower than the correlation between the expression of human genes on Hsa21 transplanted into mouse cells and their counterparts in human cells (R^2=0.90) [29], which aligns with the remote evolutionary distance between Km and Sc (**Fig. 1B**). Compared to Sc, on average, 22.7% and 18.3% of the genes in R1 and R3, respectively, were up-regulated in KS, while 27.3% and 19.3% of the genes in R1 and R3 were down-regulated in KS, respectively (FDR-adjusted $p < 0.05$ by Wald test and absolute log2FoldChange >1; **Fig. 4B, Table S3**). The median log2-fold change for up- and down-regulated genes was 1.81 and -1.57, respectively. Consistent with the case studies of *SPS22* and *FLO9*, the high proportion and fold change of differentially expressed Sc genes reflect dramatic differences in the *trans*-regulatory environment between Sc and the hybrids.

The genes showing differential expression between Sc and hybrids were in general uniformly distributed across the transferred chromosomes (**Fig. S9**), but we found a region around *HML* that showed derepression across multiple genes in KS-R3, providing an interesting example for chromatin-level regulatory divergence. The *HML* locus, along with its flanking genes *GEX1* and *VBA3*, is repressed in Sc by *SIR* complex [50]. Consistent with this previous knowledge, we found little expression of these genes in Sc (**Fig. 4C**, upper panel). Interestingly, *GEX1*, *VBA3* and *HML* genes were highly expressed in KS-R3 (**Fig. 4C**, lower panel), consistent with derepression. qPCR confirmed that the relative mRNA levels of α1 and α2 were upregulated 42-fold and 39-fold, respectively, in KS-R3 compared with Sc-R3 (**Fig. 4D**). The differential expression might be explained by different composition of

silencers between *Kluyveromyces* and *Saccharomyces* [51]. The silencer of *HML* in KS-R3 might not be able to recruit essential proteins such as Rap1 and ORC to the locus [52], contributing to the derepression of α1 and α2, and the flanking genes *GEX1* and *VBA3*.

While the expression of Sc genes underwent significant changes in the hybrids, R1 and R3 also profoundly affected the expression of Km genes. Out of 4,975 Km genes, 931 and 803 genes in KS-R1 and KS-R3, respectively, exhibited significant expression differences compared to Km-V in YPD (FDR-adjusted $p < 0.05$ by Wald test and absolute log2FoldChange >1; **Fig. 4E, Table S3**). R1 encodes a transcription factor, Oaf1, that regulates at least 97 Sc target genes [53]. Among the 73 Km orthologs of the known Sc target genes (see **Methods** for ortholog assignment), 27 (37.0%) showed differential expression in KS-R1. R3 encodes four transcription factors regulating at least 305 Sc target genes [53], with 44/160 (27.2%) of their Km orthologs differentially expressed in KS-R3 (**Table S3**). This suggests that transcription factors encoded by R1 and R3 might directly alter gene expression in Km, but a large fraction of the observed transcriptional changes might be explained by indirect or uncharacterized regulation. Under TM and NaCl stresses, the number of differentially expressed genes was substantially lower than in YPD (**Fig. 4E**, **Table S3**). These results indicate that the heterologous chromosomes induced pervasive changes in expression of the endogenous genome, potentially via novel Sc-Km regulatory interactions. Interestingly, regulation from the Km genome became dominant under stress conditions, removing much of the effects associated with foreign chromosomes found in YPD.

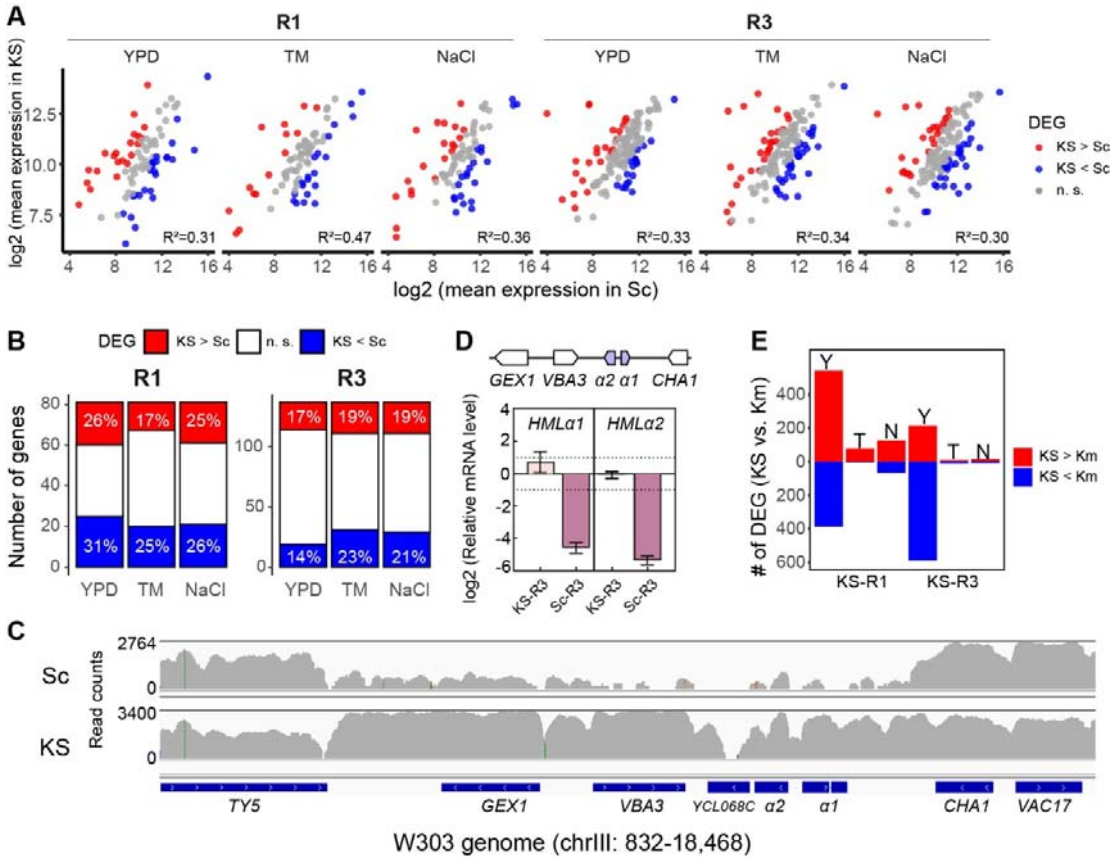

Fig. 4. Transferred Sc chromosomes were actively transcribed in the hybrids. (A) Correlation of Sc gene expression between hybrids (KS) and Sc strains. The expression level was represented by log2 (average normalized read counts). Each point represents the average of three replicates. Adjusted R^2 were derived from linear regression. N = 81 genes for R1, and 137 genes for R3 (see **Methods** for data filters). DEG, differentially expressed genes. n.s., not significant. **(B)** Number of significantly up- and down-regulated R1/R3 genes in hybrids. **(C)** Derepression of the *HML* locus in KS-R1, shown by raw read counts (grey bars) covering the *GEX1-CHA1* region in the W303 genome, visualized by Integrative Genomics Viewer. Data were from one representative biological replicate in YPD. Grey bars are in log scale. **(D)** The relative mRNA levels of *HML*α1 and *HML*α2 in KS-R3 and Sc-R3 determined by qPCR, normalized to the average of three housekeeping genes as described in **Fig. 3D**. The values represent the mean ± SD (n=3). **(E)** Number of DEGs between KS strains and Km-V. Y, YPD; T, TM; N, NaCl. In this figure, all DEGs are defined as an FDR-adjusted p-value < 0.05 by Wald test and abs(log2FoldChange) > 1.

Contributions of *cis* and *trans* effects to the expression divergence between Km and Sc

The monochromosomal hybrids provide a unique opportunity to examine the contribution of *cis*- and *trans*-regulatory divergence to the evolution of gene expression in the two remotely related species. In the hybrid, alleles from the two species are exposed to the same *trans* environment, so their expression differences stem from differences in *cis*-acting regulatory elements, such as promoters, that are physically located on the same DNA strand

of the regulated genes. Allelic expression is also regulated by *trans*-acting factors, i.e. diffusible products, such as transcription factors, that are not linked with the affected genes. The expression differences between the parental species are the sum of *cis*-and *trans*-acting effects. Therefore, subtracting the allelic differences in hybrids from parental differences yields an estimation of *trans* effects (**Fig. 5A**) [9]. In order to characterize the effects of *cis* and *trans* regulatory divergence, we identified Km orthologs for 62/85 genes on R1 and 100/156 genes on R3, with an average amino-acid sequence similarity of 48.0% (BLOSUM62-based similarity, see **Methods** and **Table S4**). Using models in DESeq2, we identified genes with significant differential expression driven by *cis*-only (parental differences completely explained by allelic differences in hybrids, upper right panel in **Fig. 5B**), *trans*-only (no allelic differences in hybrids but significant parental differences, lower left panel in **Fig. 5B**) or *cis*-and-*trans* effects (upper left panel in **Fig. 5B**, see **Methods** and **Table S5** for details; significance was based on an adjusted p-value < 0.05). Genes that showed no allelic differences in neither parents nor hybrids were classified as conserved (lower right panel, **Fig. 5B**). The genes were most commonly under both *cis* and *trans* effects (57-63%, **Fig. 5B & C**), which deviates from the previous notion that *cis* effects become increasingly dominant as species diverge [16]. However, we note that the pronounced *trans* effect could be associated with the fact that only one chromosome was transferred into the hybrids. Interestingly, when both significant, the *cis* and *trans* effects often act in the opposite direction, i.e. their effects compensate each other (blue points/bars, **Fig. 5B&C**). Only a marginal proportion of genes showed reinforcing effects, where *cis* and *trans* effects act in the same direction (magenta points/bars, **Fig. 5B&C**). The prevalence of compensatory effects was also supported by negative correlations between *cis* and *trans* effects across treatments (**Fig. 5D**). The data together suggest that stabilizing selection on gene expression might operate on a much longer evolutionary distance than previously appreciated.

Across environmental conditions, the correlations within *cis* effects (average of 0.85) and *trans* effects (average of 0.79) were high, indicating that the mechanisms causing expression divergence under different conditions were similar (**Fig. 5D**). The lower correlation among *trans* effects suggests that *trans* effects were more likely to be environmental-dependent than *cis* effects, aligning with previous results from intragenus hybrids [11].

What factors could potentially drive divergence in *cis*- and *trans*-regulation of different genes? We considered (1) essentiality of genes [54] and (2) gene duplication [55]. After separating from Km, Sc underwent whole-genome duplication (WGD), leading to paralogs in

Sc genome (**Fig. 1A**). We reasoned that essential genes might be less likely to evolve regulatory changes due to functional constraint. On the other hand, genes with paralogs might be more likely to exhibit regulatory divergence due to redundancy. We found that the average magnitude of *cis* effects, but not *trans* effects, was significantly lower in essential genes than dispensable genes ($p = 0.036$, Wilcoxon test, **Fig. 5E**). This suggests that *cis* effects might play a greater role than *trans* effects in driving divergence among non-essential genes [56]. We did not find any significant correlations that distinguish genes with and without paralogs.

Finally, we note that the monochromosomal hybrids' *trans* environment predominantly resembled Km (**Fig. S10**), given that the transferred R1 and R3 chromosomes contained only a small number of genes. As shown above, the pervasive expression changes in Sc genes upon chromosomal transfer reflected the divergence in *trans*-acting factors between Km and Sc. We expect that the change in *trans* environment would cause a more dramatic effect on Sc-specific genes that evolved after the split of the Sc and Km lineages. There were 56 Sc-specific genes in R1 and R3 that did not have any identifiable orthologs in Km (**Table S6**). Indeed, the magnitude of expression differences between hybrids and Sc was significantly greater for Sc-specific genes than genes with orthologs ($p = 0.01$, Wilcoxon test; **Fig. 5F**). This potentially suggests that regulation of Sc-specific genes required co-evolution of *trans*-acting factors in a lineage-specific manner.

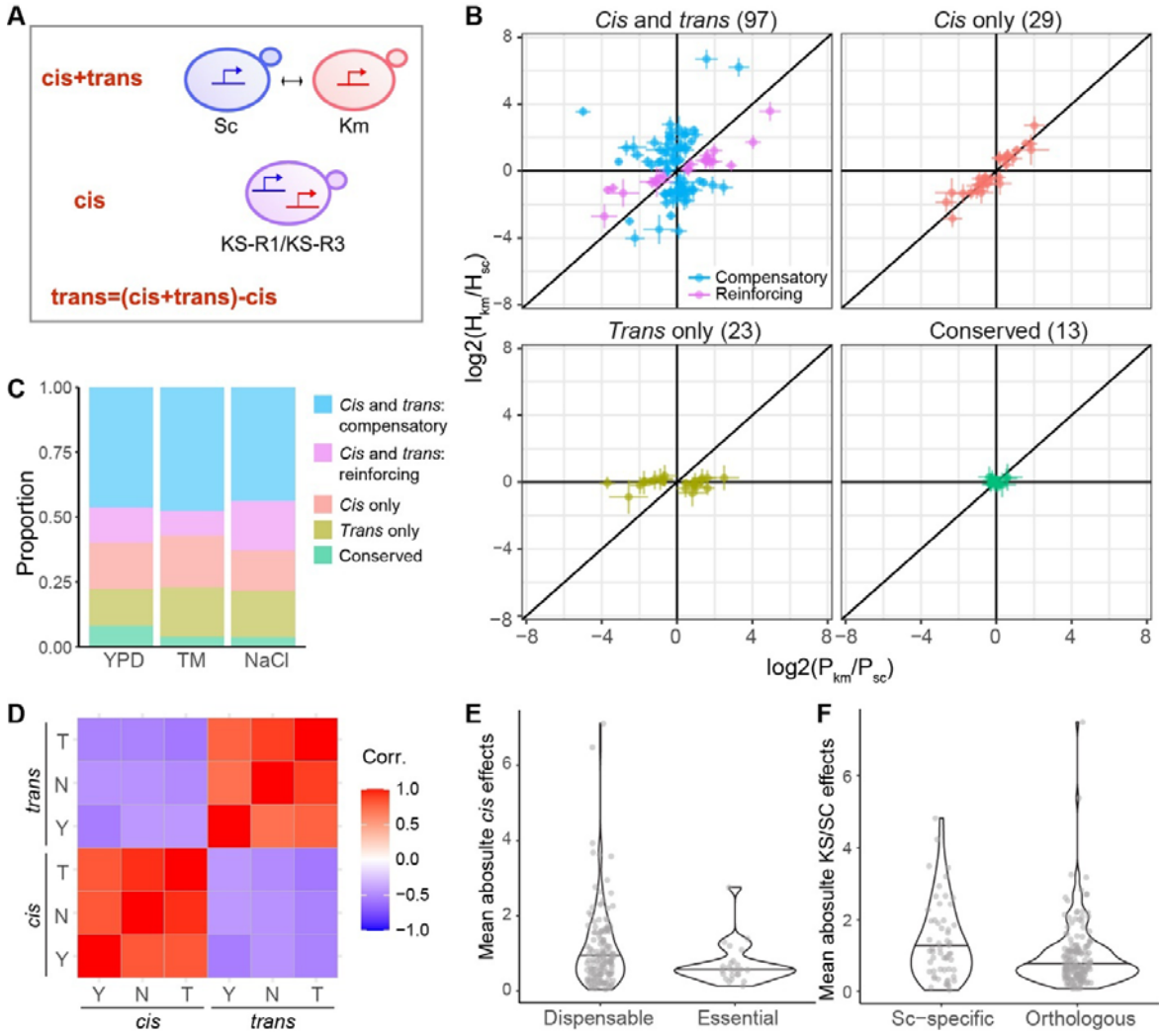

Fig. 5. Contributions of *cis* and *trans* effects to the expression divergence between Km and Sc. (A) Schematic representation of *cis* and *trans* effects in expression divergence between Km and Sc. **(B)** Log2 fold changes between alleles in hybrids (H) vs. parental differences (P), adjusted with the ashr method. Error bars represent 95% confidence interval. Numbers in the parentheses indicate the number of genes. Data are from the YPD treatment. (**C**) Proportion of genes showing *cis* only, *trans* only, *cis* & *trans*, compensatory, and reinforcing effects in three conditions. **(D)** Pearson correlation coefficient (Corr.) between *cis* and *trans* effects across conditions. Data are average correlations of three replicates, using a cross-replicate design. YPD (Y), TM (T), NaCl (N). **(E)** The magnitude of *cis* effects on essential genes and dispensable genes, averaged across three treatments. **(F)** The magnitude of log2 (KS/Sc) expression differences in Sc-specific genes and orthologous genes, averaged across three conditions. Log2 fold changes were adjusted with the ashr method. Midlines in the violin plots in (**E**) and (**F**) represent median.

Discussion

Interspecific hybridization often leads to novel phenotypes that are of interest for industrial purposes and evolutionary studies. For diverged species that cannot mate naturally, artificial chromosomal transfer provides an opportunity to explore the molecular and

phenotypic consequences of combining genetic materials evolved independently during millions of years of evolution. In this study, we, for the first time, successfully introduced chromosomes of *S. cerevisiae* to *K. marxianus*, two species both with great industrial potential but genetically as diverged as human and lancelet (**Fig. 1B**). We show that the transferred Sc chromosomes are stably maintained in Km. The monochromosomal hybrids exhibited heterosis, demonstrating the technology's potential in future phenotypic screens. The improved salt resistance and flocculation phenotypes were associated with Sc promoters being activated by Km-encoded *trans*-acting factors in the artificial hybrids, to a greater level than the native regulation in Km or Sc. Finally, we examined the molecular consequences of monochromosomal hybridization with transcriptomic analysis, revealing broad transcriptional responses upon chromosomal transfer, as well as prevalent compensatory evolution of *cis*- and *trans*-regulatory changes during the divergence of the two species.

One of the technological advances in our study is the method to enable stable maintenance of Sc chromosomes in Km. There are several technical factors of consideration. First, we removed Sc TELs and circularized the chromosomes of interest. The circularization made it possible to easily remove unwanted linear chromosomes by exonuclease treatment [40], which may increase transformation efficiency. In the case of *CEN* engineering, it was important to ensure that the heterologous *CEN* was not partially functional, which has been shown to disrupt chromosome segregation and lead to dicentric breakage, thereby causing genome rearrangements and instability [57]. We found that Sc and Km *CEN*s were non-functional in the other species. Therefore, we may use double *CEN*s for maintaining the heterologous chromosomes. Next, we considered the density of *ARS*s. The requirement of *ARS* density for YACs varied in previous reports, from one *ARS* per 30 kb [58], 51 kb [59], to 1 Mb [60]. In our study, *KmARS1* was positioned at a density of one *ARS* per 110 kb in R1 and 150 kb in R3, which proved to be sufficient for replication of Sc chromosomes in the hybrid. Finally, our strategy allows for possibilities of transferring multiple chromosomes into Km. This can be done either by marker recycling, i.e., popping out *URA3* in the monochromosomal hybrid (see the sequences in **Supplementary Data File 1**) and transforming another chromosome subsequently, or by mating with another monochromosomal hybrid.

There are a few advantages in constructing functional monochromosomal hybrids for synthetic biology purposes. First, it partly circumvents the problem of genome incompatibility, which is a major barrier for hybridization between remotely related species. We found that, although Km and Sc cannot form hybrids, the monochromosomal hybrids

with R1 or R3 were viable. It suggests that R1 and R3 did not carry incompatibilities that are detrimental to the hybrids' survival, although they may cause fitness defects under certain environmental conditions (**Fig. 3A**). These observations imply that R1 and R3 might carry environment-dependent incompatibility, which should be noted in future studies. Second, the hybrids exhibited heterosis in a few phenotypes, demonstrating industrial potential. They also provide ideal materials for directed evolution for desirable traits, as demonstrated by other synthetic hybrids [61]. Third, the limited number of genes in the transferred chromosomes made it easier to identify the molecular basis of phenotypes of interest. We found that the flocculation phenotype in KS-R1 was due to overexpression of *ScFLO9*, consistent with its known role in Sc [62]. The heterosis in NaCl tolerance stems from overexpression of *ScSPS22* in KS-R3, which might be caused by loss of repressors [63]. It remains to be understood why overexpression of *ScSPS22* had an opposite effect in KS than Sc. One explanation lies in the different composition of glucan in cell wall between Km and Sc [64]. As a gene responsible for synthesizing β-1,3-glucan in the cell wall, *ScSPS22* might affect the two species differently under osmotic stresses.

The synthetic Km-Sc monochromosomal hybrids showed interesting phenotypic and molecular characteristics, demonstrating that chromosome transfer is functional, even across a remote evolutionary distance such as between yeast genera. Previous interspecific chromosomal transfers in yeast have been successful in using *S. cerevisiae* as a container to maintain heterologous genetic materials from bacteria [30,60,65,66], but little interaction between the host and the heterologous chromosomes has been characterized, or desired at all. In our study, we found that the Sc chromosomes were "alive" in the Km background. Genes on the transferred R1 and R3 chromosomes were actively transcribed, despite a high level of sequence divergence. Genes on R1 and R3 showed significant expression differences between KS and Sc backgrounds, and the same for Km genes between KS and Km background. The transcriptional responses indicate active interspecific regulation, which can give rise to heterosis phenotypes, as shown with *SPS22* and *FLO9*. It is of future interest to investigate what proportion of the regulatory interactions between the two species' genomes are associated with beneficial phenotypes, or, on the other hand, indicative of molecular incompatibility.

The monochromosomal hybrids allowed for exploring evolutionary patterns of gene regulation between distantly related species. We found that the intergeneric expression differences were primarily driven by a combination of *cis* and *trans* effects (**Fig. 5B, C**), contrasting with previous findings with intrageneric species where expression divergence was

mainly attributed to changes in *cis* effects [11,16]. However, we note that the monochromosomal hybrids differ from allodiploid hybrids in that its *trans* environment closely resembles one of the parental species (Km in this case), but are similar to introgression lines where only parts of the genomes are hybridized [67,68]. Therefore, the Sc and Km alleles experienced imbalanced changes in *trans* environment, potentially leading to an overestimation of *trans* effects. With this deviation in mind, our conclusion is consistent with previous studies showing that *cis*-*trans* coevolution is more likely to accumulate over greater evolutionary timespans than *cis* or *trans* effects alone [69]. Additionally, the prevalence of compensatory effects of *cis* and *trans* changes (**Fig. 5C**) is consistent with stabilizing selection on gene expression [11,16], demonstrating that stabilizing selection is able to operate on an evolutionary timescale of over a hundred million years. Future studies with even more diverged species may help us to understand what is the upper limit of evolutionary distance for stabilizing selection to act on and how the relative contribution of *cis* and *trans* effects change across evolutionary timescales.

In summary, our study established a strategy for engineering the structural elements and ARS of a functional chromosome before transferring it between intergeneric yeasts. This strategy might be extended to other microbes as well as to plants. The resultant hybrids, containing rationally designed synthetic genomes, provide valuable resources for cell factories, synthetic biology, and evolutionary genomics.

Materials and Methods

Strains and media

Yeast strains used in this study are listed in **Table S7**. Sc strain W303-1A (*MATa leu2-3,112 trp1-1 can1-100 ura3-1 ade2-1 his3-11,15*) was subjected to chromosome engineering. The engineered Sc chromosome was transferred into a *ura3Δ* Km strain, FIM-1ΔU [70]. The following media were used in this study: YPD [71], synthetic medium lacking uracil or leucine (SD-Ura or SD-Leu) (0.17% yeast nitrogen base without amino acids and ammonium sulfate, 2% glucose, 1 g/L sodium glutamate, 2 g/L DO Supplement-Ura (630416, Takara) or DO Supplement-Leu (630414, Takara), 2% agar for plates), SD (same recipe as SD-Ura, with the addition of 20 mg/L uracil), and ME (2% malt extract, 3% agar). G418 (A600958, Sangon) and hygromycin (H8080, Solarbio) were added to YPD medium at final concentrations of 200 mg/L and 300 mg/L, respectively, to prepare YPDG and YPDH media. Both antibiotics were supplemented into YPD and SD-Ura to prepare YPDGH and SD-Ura+GH, respectively. Unless otherwise indicated, cells were grown at 30 □.

Plasmids

All plasmids used in this study are listed in **Table S8**. All primers are listed in **Table S1**. A previously published vector LHZ626 which contains CEN and ARS elements from both Sc and Km (double CEN/ARS plasmid), as well as *KmURA3*, served as a control for circular chromosomes [41]. To construct plasmids for diploid selection, a fragment containing *ScARSH4* and *ScCEN6* was amplified from LHZ626 and inserted into the HpaI and SpeI sites of a Km-centromeric plasmid, LHZ882 [72], yielding LHZ1493. KANMX6 (kan^R) was amplified from pFA6a-KANMX6 and used to replace HPHMX4 (hyg^R) in LHZ1493 to produce LHZ1494. To create plasmids with different combinations of ARS and CEN from Km and Sc, a BamHI site was introduced between *KmARS1* and *KmCEN5* of LHZ882 to generate LHZ1495. *ScCEN6* was inserted between the BamHI and SalI sites of LHZ1495 to generate LHZ1496. *ScARSH4* was inserted between the BamHI and HindIII sites of LHZ1495 to generate LHZ1497. *ScARSH4* and *ScCEN6* were inserted between the HindIII and SalI sites of LHZ1495 to obtain LHZ1498. *KmARS18* and *KmCEN3* were inserted between the HindIII and SalI sites of LHZ1495 to obtain LHZ1783. *ScARS1* and *ScCEN4* were inserted between the HindIII and SalI sites of LHZ1783 to obtain LHZ1784. *ScARS1* was inserted between the BamHI and HindIII sites of LHZ1783 to generate LHZ1785. *ScCEN4* was inserted between the BamHI and SalI sites of LHZ1783 to generate LHZ1786. *ScARS1* and *ScCEN4* were inserted into the SalI site of LHZ1783 to obtain LHZ1787.

In order to remove the telomeres and join the chromosomal ends, we first constructed CRISPR plasmids expressing single guide RNAs (gRNAs) targeting telomeres of each end of chr1 and chr3. Primers containing a 20 bp gRNA sequence were annealed in pairs and inserted into the SapI sites of pRS425-Cas9-2xSapI, resulting in plasmids LHZ1499A, B, LHZ1500A and B. Next, the gRNA cassette from LHZ1499A was inserted into the NotI site of LHZ1499B to produce LHZ1499. Similarly, the gRNA cassette from LHZ1500A was inserted into the NotI site of LHZ1500B to produce LHZ1500. The double-gRNA plasmids, LHZ1499 and LHZ1500, were subsequently transformed into yeast (see below). In order to insert *KmARS1* and *KmCEN5* into the circularized chromosomes, we cloned gDNAs into the SapI sites of pRS425-Cas9-2xSapI to construct LHZ1501∼1504, following the same cloning procedure as described above. The homologous repair templates (“donor DNA”, see below) used in CRISPR/Cas9 genome editing was assembled into pMD-18T with In-Fusion Snap Assembly (Clontech), according to the designs in **Supplementary Data File 1**.

For flocculation analysis, the *ScFLO9* cassette, including 1000 bp upstream, the ORF of *ScFLO9*, and 200 bp downstream sequence was amplified from the genome of W303-1A.

This cassette was inserted into the NotI site of LHZ626 to produce LHZ1505, and into the SmaI and SpeI sites of pRS315 and pRS425 to produce LHZ1509 and LHZ1510, respectively.

For NaCl tolerance analysis, the *ScSPS22* cassette, including 1000 bp upstream sequence, the ORF of *ScSPS22*, and 200 bp downstream sequence was amplified from the genome of W303-1A. This cassette was inserted into the NotI site of LHZ626 to produce LHZ1506, and into the SmaI and SpeI sites of pRS315 and pRS425 to produce LHZ1511 and 1512, respectively. The 1000 bp upstream sequence of *ScSPS22* in LHZ1506 was replaced by the 1000 bp upstream sequence of *KmSPS22* to produce LHZ1507. The *KmSPS22* cassette, including 1000 bp upstream sequence, the ORF of *KmSPS22*, and 200 bp downstream sequence was amplified from the genome of FIM-1ΔU and inserted into the NotI site of LHZ626 to produce LHZ1508. The full sequences of LHZ626, LHZ1495, and pRS425-Cas9-2xSapI are listed in **Table S8**.

Transformation efficiency and plasmid stability

Fim-1ΔU and W303-1A were grown in YPD liquid medium overnight. Cells from 1 mL-culture were pelleted and transformed with LHZ626, LHZ1495~LHZ1498, respectively, using the lithium acetate (LiAc) method [73,74]. The cells were diluted and spread onto YPDH plates. Colony-forming units (CFUs) were counted after 3 days. The transformation efficiency (CFUs/μg DNA) was calculated taking the dilution factor into account. To measure the stability of the plasmid, transformants were grown in YPD liquid medium for 24 h. The cells were then diluted and spread onto YPD and YPDH plates. Stability was determined by dividing the CFU count on YPDH plates by that on YPD plates. The experiments were replicated three times.

Mating assay

The quantitative mating assay was performed as previously described [75] with modifications. Strains transformed with LHZ1493 (hyg^R) were used as experimental cells, and strains transformed with LHZ1494 (kan^R) served as tester cells. Both experimental and tester cells were cultured overnight in YPDH and YPDG liquid media, respectively. Cells were then washed and resuspended in H_2O to an OD_{600} of 1. A total of 100 μL of experimental cells was mixed with 500 μL of tester cells. The mixture resulted in a 1:5 ratio of experimental to tester cells when both cell types were Km or Sc. The mixture resulted in a 1:10 ratio of Sc experimental cells to Km tester cells, as CFU per OD_{600} of Km cells was twice that of Sc cells. The mixed cells were pelleted, resuspended in 20 μL of ddH_2O, and spotted onto ME plates. After incubation at 30 □ for 24 h, cells were washed off the ME plates with ddH_2O and then pelleted and resuspended in 1 mL of ddH_2O. To visualize the

mating result, a total of 3 μL cells were spotted on YPDH, YPDG, and YPDGH (Fig.1E). These plates were incubated at 30 □ for 24 h. To quantify mating efficiency, the cells were diluted and plated onto YPD and YPDGH plates. The mating efficiency was calculated as the number of colonies on YPDGH plates divided by one-sixth of the number on YPD plates, reflecting the 1:5 ratio of experimental to tester cells. The experiments were replicated three times.

Engineering of Sc chromosome I and III

Each step of engineering Sc chromosome I (chr1) or III (chr3) involved transforming a CRISPR plasmid (**Table S8**) and a donor, which is a PCR product for homologous recombination repair. The composition and full sequences of the donors are listed in **Supplementary Data File 1**.

Chr1 and chr3 were circularized as previously described [76]. First, LHZ1499 or LHZ1500 was transformed into W303-1A to induce double strand breaks in both telomeres in chr1 or chr3. A DNA fragment "chr1-cir" or "chr3-cir" containing *KmURA3* with homologous arms to the chromosomal ends was simultaneously transformed to connect the two chromosomal ends with *KmURA3*. The constructs above were designed to remove the left telomere (0-1111 bp) and the right telomere along with the repetitive sequence (208917-252221 bp) of chr1, and the left telomere (0-831 bp) and the right telomere (334198-341087 bp) of chr3. Successful circularization was selected by SD-Ura-Leu medium. The transformants with circularized chromosomes were named Sc-ring1 and Sc-ring3.

In order to insert *KmARS1* and *KmCEN5* into the circularized chromosomes, we transformed LHZ1501 and a donor "chr1-ARS1" into Sc-ring1 to insert *KmARS1* and hyg^R at 66090 bp of chr1, resulting in a strain named Sc-ring1L. LHZ1502 and a donor "chr1-ARS1/CEN5" were transformed into Sc-ring1L to insert *KmARS1*/*KmCEN5* and kan^R at 157346 bp of chr1, resulting in a strain named Sc-R1. Similarly, LHZ1503 and a donor "chr3-ARS1/CEN5" were transformed into Sc-ring3 to insert *KmARS1*/*KmCEN5* and hyg^R at 108718 bp of chr3, resulting in a strain named Sc-ring3L. LHZ1504 and a donor "chr3-ARS1" were transformed into Sc-ring3L to insert *KmARS1* and kan^R at 243183 bp of chr3, resulting in a strain named Sc-R3. All transformations described above followed the LiAc method [73,74].

Extraction and protoplast transformation of R1 and R3

R1 and R3 were extracted from Sc-R1 and Sc-R3 as previously described [40], which was developed for purifying yeast artificial chromosomes up to 600 kb in size. A total of 10 μL R1 or R3 was transformed into Km by protoplast transformation [42]. The transformants were selected on SD-Ura+GH plates.

Pulsed-Field Gel Electrophoresis (PFGE)

Plugs containing the genome of Sc, Km, and hybrid cells were prepared by using the CHEF Yeast Genomic DNA Plug Kit (170-3593, Biorad). To separate circular R1 from linear chromosomes in KS-R1, chromosomes were separated on the CHEF MAPPER^{TM} XA System in a 1% pulsed field certified agarose gel (162-0137, Biorad) in 0.5×TBE (diluted from 10×TBE, T1051, Solarbio) at 14 □. The running time was 24 h at 6.0 V cm^{-1}, with a 60~120 sec switch time ramp at an included angle of 120 °. The plug containing the entrapped R1 was cut out and linearized with NotI as described in the protocol of the CHEF Yeast Genomic DNA Plug Kit. Similarly, R3 in KS-R3 was separated from linear chromosomes and then linearized with AscI. Chromosomes of W303-1A, Sc-R1, Sc-R3, linearized R1 and R3 were separated in a 1% pulsed field certified agarose gel in 0.5×TBE at 14 □. The running time was 16 h at 6.7 V cm^{-1}, with a 10~40 sec switch time ramp at an included angle of 120 °. Lambda PFG Ladder (N0341S, NEB) was used as a size marker for PFGE.

Growth curves of KS-R1 and KS-R3 and the stabilities of transferred chromosomes

As a control, Fim-1ΔU was transformed with LHZ626 to produce Km-V. KS-R1, KS-R3, and Km-V were cultured in YPDGH liquid medium overnight. The overnight culture (referred to as day 0 culture) was diluted into YPD liquid medium to an initial OD_{600} of 0.2 and grown at 30 □. To monitor growth curves, the OD_{600} of the culture was recorded every 2 hours for the first 14 hours. To assess the stability of the transferred chromosomes, the culture was diluted into fresh YPD medium to start at an OD_{600} of 0.2 every 24 hours, a period corresponding to approximately 7 generations. Cultures from day 0 and after 5 days of growth were diluted and plated onto YPD and YPDGH plates on the day the cultures were collected. Stability was determined by dividing the CFU count on YPDGH plates by that on YPD plates. The loss rate of transferred chromosomes per generation was calculated as previously described [72]. The experiments were replicated three times.

Genome Sequencing

Km-V, Sc-R1, Sc-R3, KS-R1, and KS-R3 were cultured overnight in SD-Ura+GH liquid medium. The cultures were diluted to an OD_{600} of 0.2 and cultured until the OD_{600} reached 0.6. The cells were collected and washed once with ddH_2O. Genomic DNA was extracted using the E.Z.N.A. Fungal DNA Kit (D3390, OMEGA Bio-Tek) and sequenced on the Illumina NovaSeq 6000 platform using the 150-bp pair-end sequencing strategy (BIOZERON, Shanghai, China).

To construct the reference sequences for R1 and R3, sequences of chr1 and chr3 were extracted from the W303-1A genome (GenBank assembly: GCA002163515.1). We then

manually modified the sequences to reflect our genome edits, including the insertions of Km elements and deletions of telomere sequences, giving rise to reference sequences R1 and R3 (provided in **Table S1**). Annotations for R1 and R3 were transferred from S288c annotations with SnapGene. The whole-genome sequencing data were processed by BIOZERON biotechnology. To identify *de novo* variants during circular chromosome transfer, the raw sequencing data of Sc and KS strains were aligned to reference sequences for R1 or R3 using BWA [77] with default settings. Picard tools were used to remove PCR duplicates. The average sequencing depth of KS-R1, Sc-R1, KS-R3, and Sc-R3 was 298, 1,183, 1,241 and 1,134 for the respective R1 or R3 chromosome. SNPs and indels were called following the best practices of GATK HaplotypeCaller [78]. Then, all heterozygous variants were removed from the VCF files of KS-R1 and KS-R3. All variants coexisting in both KS-R1 and Sc-R1 or KS-R3 and Sc-R3 were filtered out from the KS-R1 and KS-R3 VCF files as well. The remaining variants were considered to have occurred during the chromosome transfer. In the case of R1, no *de novo* mutation was found.

To identify variants in the genome of Km, raw sequencing data of KS-R1, KS-R3, and Km-V were aligned to the reference genome of FIM1 (GenBank assembly: GCA_001854445.2) [79] combined with either R1 or R3 sequence, using BWA with default parameters. Picard tools were used to remove PCR duplicates. The average sequencing depth for KS-R1, KS-R3 and Km-V was 1,036, 1,102 and 615, respectively. GATK HaplotypeCaller was used to identify the variants in these strains, following its best practices. VCFtools [80] was used to remove variants shared between Km-V and KS-R1 or KS-R3, as well as heterozygous calls. The remaining unique, homozygous variants in KS-R1 and KS-R3 were listed in **Table S2**.

RNAseq and qPCR

Three biological replicates of Km-V, Sc-R1, Sc-R3, KS-R1, and KS-R3 were cultured overnight in SD-Ura+GH liquid medium. The cultures were diluted into YPD to achieve an OD_{600} of 0.2. Once the OD_{600} of the cultures reached 0.6, cells were collected directly for the YPD treatment. For stress treatment, the culture was supplemented with tunicamycin (T8480, Solarbio) at a final concentration of 1 μg/mL, or with NaCl at a final concentration of 1 M, and cells were collected after 1 hour. Total RNA was extracted using the ZR Fungal/Bacterial RNA MiniPrep kit (R2014, ZymoResearch). Samples were reversed transcribed using TruSeqTM RNA sample preparation Kit (Illumina, California, USA) and sequenced by Illumina HiSeq X Ten (BIOZERON, Shanghai, China). Batch information was provided in **Supplementary Data File 2**.

The reads were mapped to corresponding reference genomes with BWA (0.7.17-r1188) [77] under the default settings. Different reference genomes were used for different samples: Km-V samples were mapped to the FIM1 genome (GCA_001854445.2), *S. cerevisiae* samples were mapped to a W303 genome [81] (GCA_002163515.1, ScRAPdb[82] code W303.asm02.HP0), and KS samples were mapped to a combined genome of FIM1 and chrI and chrIII of W303. They were then processed with samtools [83] to remove duplicated reads. Reads with mapping quality lower than or equal to 2 were also removed with samtools, as well as those with 30 or more soft-clipped bases. The number of reads mapped to each allele (with a minimal mapping quality of 10) was counted with htseq-count [84], with the setting "-idattr ID -t CDS". Counts from exons were summed up to generate counts per gene. The gene models for the RNA-seq analysis were based on the W303.asm02.HP0 annotation downloaded from ScRAPdb. There are 5,680 annotated genes in this genome, but not all genes were annotated to a known systematic name as in the S288C genome, due to known intraspecific variation [81]. We performed an all-vs-all BLAST search between W303 and S288C genes (R64 assembly) and selected the top S288C hit for each W303 gene, based on E-value and query coverage. 5,347 out of the 5,680 (94%) W303 annotations matched S288C genes unambiguously. The rest W303 gene models were kept in the analysis but flagged with "ambiguous" in the dataset.

Differential expression was analyzed with DEseq2 [85]. To examine changes in expression levels before and after chromosomal transfers (Sc vs. KS; Km vs KS), the data were fitted to a model of *count ~ group*, where *group* represented a combination between the strain factor (Sc/KS/Km) and the treatment factor (YPD/TM/NaCl). In the Sc analysis (**Fig. 4A to D**), R1 and R3 data were treated separately. Data from different treatments were combined in one data frame and normalized together. In the Km analysis, data from KS-R1, KS-R3 and Km-V across three treatments were combined and normalized together. Genes with an average read count lower than 5 of any *group* were removed from the analysis, leaving 218 out of 241 Sc genes (chrI and chrIII) and 4,975 out of 5,081 Km genes in the dataset. The median of read counts across groups was 1,413 for Sc genes and 1,267 for Km genes, prior to normalization. Adjusted p-values for pairwise comparisons between *groups* (e.g. Sc-YPD vs. KS-YPD) were derived from FDR-corrected Wald significance tests, with an FDR cutoff of 0.05. Log2 fold changes were shrunken with the ashr method [86]. Differentially expressed genes (DEG) were defined as an adjusted p-value lower than 0.05 and an absolute log2 fold change higher than 1.

For qPCR, RNA samples were reverse-transcribed using a PrimeScript RT Reagent Kit (RR037A, Takara, China). The qPCR was performed using ChamQ Universal SYBR qPCR Master Mix (Q711-02, Vazyme). The mRNA level was normalized to the average of three housekeeping genes, including *MPE1*, *TRK1*, and *SWC4*. Primers used in qPCR are listed in **Table S1.**

***Cis* and *trans* effects**

Orthologs were identified with OrthoFinder (3.0.1b1)[36]. Animo acid sequences of six species were provided to OrthoFinder, including *S. cerevisiae* (W303, GenBank #GCA_002163515.1), *K. marxianus* (FIM1, GCA_001854445.2), *Candida albicans* (SC5314, GCF_000182965.3), *Lachancea thermotolerans* (CBS6340, GCF_000142805.1), *Naumovozyma castellii* (CBS4309, GCF_000237345.1), and *Torulaspora delbrueckii* (CBS1146, GCF_000243375.1), along with a species tree according to Shen et al. (2018) [31]. There was a total of 32,488 genes across the six genomes, 93.5% of which were placed into orthogroups. There was a total of 5,056 orthogroups, of which 3,630 were with all species present and 2,847 were single-copy orthogroups. When focusing on single-copy orthologues, the median of amino acid sequence similarity between *S. cerevisiae* and *K. marxianus* genes was 51.0% (using BLOSUM62 scoring matrix), between that of *S. cerevisiae-T. delbrueckii* (58.7%) and *S. cerevisiae-C. albicans* (37.0%), consistent with expectation (**Fig. S11A**). The high level of evolutionary divergence resulted in loss of synteny (**Fig. S11B**), so we did not further take into account of synteny in the ortholog analysis.

Between *S. cerevisiae* and *K. marxianus*, there were 4,851 orthologs, of which 3,813 were one-to-one orthologs. In the cases where multiple orthologs were identified for one gene (one-to-many or many-to-one) and many-to-many orthologous relationships, we performed pair-wise sequence alignments within the orthogroup and selected the reciprocal best match based on amino-acid sequence similarity, identifying 4,330 orthologous pairs. The median amino acid sequence similarity was 48.4%. The length of orthologs did not differ by more than two fold for 4,149/4,330 (95.8%) orthologous pairs, ruling out partial match due to local similarity. The orthologous genes were listed in **Table S4**.

Cis and *trans* effects were calculated with DESeq2 as previously described [17]. R1 and R3 data were combined. YPD, TM and NaCl data were analyzed separately. Out of 241 genes on chrI and chrIII of W303 genome, we identified Km orthologs for 173 genes, 162 of which had an average read count above 5 across replicates and were retained in the analysis. We designated Km alleles in Km-V as kmk, Sc alleles in Sc-R1 or Sc-R3 as scs, Km alleles in hybrids as hyk, and Sc alleles in hybrids as hys. The variables *gb*, *F*, and *allele* were used,

where *gb* represents genetic background (Km for kmk, Sc for scs, hybrid-Km for hyk, hybrid-Sc for hys), *F* represents generation (F0 for kmk and scs, F1 for hyk and hys), and *allele* indicates the allele (km for kmk and hyk, sc for scs and hys). The model "*count* ~ *gb*" was used for testing the significance of *cis*+*trans* and *cis* effect, i.e., contrasts between kmk and scs for *cis* + *trans* effects and between hyk and hys for *cis* effects. P-values were from Wald test followed by an FDR-correction. Log2 fold changes were adjusted with the ashr method. For testing *trans* effects, another model "*count* ~ *F* + *allele* + *F*:*allele*" was used. Significant *trans* effect was determined by a likelihood ratio test (test = "LRT", reduced = "*F* + *allele*") for testing the effect of the interaction term "*F*:*allele*".

Genes with significant *cis* or *trans* effects were defined by an FDR-adjusted p-value less than 0.05. "*Cis* only" genes were defined as significant for *cis* effects but not *trans* effects, and *vice versa*. "*Cis* and *trans*" genes include two categories: (1) genes that were significant for "*cis*+*trans*" effects as indicated by the *count* ~ *gb* model above; (2) genes that were significant for both *cis* and *trans* effects (but not necessarily significant for "*cis*+*trans*" effects, because compensatory evolution might have resulted in conserved expression between parental strains).

In order to properly address the correlation between *cis* and *trans* effects (**Fig. 5D**), we employed a cross-replicate design for deriving the *trans* effect, as previously suggested [87]. In this analysis, *cis*, *trans*, and *cis*+*trans* effects were independently calculated for each replicate (*i* = 1,2,3): $Cis_{rep_i} = log2(\frac{hyk_{rep_i}}{hys_{rep_i}})$, $Ct_{rep_i} = log2(\frac{kmk_{rep_i}}{scs_{rep_i}})$, and $Trans_{rep_i} = Ct_{rep_i} - Cis_{rep_{i+1}}$, where *Ct* denotes *cis*+*trans* effect. Then, Pearson correlation between *cis* and *trans* effects for each replicate was calculated. The correlation coefficient was averaged across the three replicates. Results are provided in **Table S5**.

In order to understand the major source of variance among the factors *allele*, *F*, and *treatment*, we performed a PCA analysis (**Fig. S10**) with TM and NaCl data combined and normalized together (YPD was excluded due to batch effect). The normalized data were transformed with the VarianceStabilizingTransformation function in DESeq2 prior to the PCA analysis.

Spot assay and quantification of growth phenotypes under various conditions

Km-V, Sc-R1, Sc-R3, KS-R1, and KS-R3 were cultured overnight in liquid SD-Ura+GH medium. The cultures were diluted to an OD_{600} of 1.0 and subjected to five serial 5-fold dilutions. These dilutions were spotted on plates using a 48-pin replicator. To evaluate the growth in different carbon sources, we used YP in combination with 2% ethanol, 3%

glycerol, or different concentrations of glucose (0.02%, 1%, 3%, and 5%). To evaluate the growth in various nitrogen sources, we replaced 1 g/L sodium glutamate in the SD medium with 1 g/L threonine, 1 g/L serine, or 1.25 g of ammonium sulfate (1/4 N). In the condition of 1/2 AA and 1/2 N, the amino acids supplemented in the SD medium were halved, and 2.5 g/L ammonium sulfate was added. In the plates for chemical treatment, YPD medium was supplemented with 0.08% H_2O_2, 60 mM acetic acid (AcOH), 0.4 μg/mL TM, 20 mM DTT, 15 μg/mL 5-FU, 1 M NaCl, 1 M sorbitol, 20 μg/mL benomyl (BML), 10 μg/mL thiabendazole (TBZ), 0.05 M hydroxyurea (HU), 0.01% methyl methane sulfonate (MMS), 5 μg/mL camptothecin (CPT), or 0.05 μg/mL cycloheximide (CHX). The plates were incubated at 30 □ or at other specified temperatures for 1-3 days before the pictures were taken. To quantify growth phenotypes, spot quantification was performed using the 'gitter' package [88] in R, with the dilution factor taken into account. The quantified spot value of a strain under a specific condition was divided by the value of the same strain grown in YPD, to calculate the relative growth value under that condition. Each spot value represents the average of three replicates.

To perform spot assays of cells with plasmids expressing *SPS22*, Sc-R3 was transformed with LHZ1511 or LHZ1512, and Fim-1ΔU was transformed with LHZ1506, LHZ1507, or LHZ1508. Transformants were cultured overnight in SD-Leu medium. The culture was diluted and spotted onto plates with or without 1 M NaCl, as described above.

Flocculation analysis

Km-V, KS-R1, and Sc-R1 were cultured overnight in SD-Ura medium. Sc-R1 was transformed with LHZ1509 or LHZ1510. Fim-1ΔU was transformed with LHZ1505. Transformants were cultured overnight in SD-Leu medium. Cells were harvested and washed with ddH_2O and 250 mM EDTA. After two subsequent washes with ddH_2O to ensure complete removal of EDTA, cells equivalent to an OD_{600} of 40 were pelleted and resuspended in 2 mL of ddH_2O in a 15 mL tube. A total of 100 μL of 1 M Tris-HCl (pH 7.5) was added to the cell suspension, followed by 1 min of agitation. The tube was then left undisturbed, and pictures were taken every minute for a total of 5 minutes. Supernatant samples were collected at various time points from the surface for OD_{600} measurement to quantify the flocculation progress.

References

1. Soucy, S.M., Huang, J., and Gogarten, J.P. (2015). Horizontal gene transfer: building the web of life. Nat. Rev. Genet. *16*, 472–482. https://doi.org/10.1038/nrg3962.

2. Steensels, J., Gallone, B., and Verstrepen, K.J. (2021). Interspecific hybridization as a driver of fungal evolution and adaptation. Nat. Rev. Microbiol. *19*, 485–500. https://doi.org/10.1038/s41579-021-00537-4.

3. Stegemann, S., Keuthe, M., Greiner, S., and Bock, R. (2012). Horizontal transfer of chloroplast genomes between plant species. Proc. Natl. Acad. Sci. *109*, 2434–2438. https://doi.org/10.1073/pnas.1114076109.

4. Ma, L.-J., van der Does, H.C., Borkovich, K.A., Coleman, J.J., Daboussi, M.-J., Di Pietro, A., Dufresne, M., Freitag, M., Grabherr, M., Henrissat, B., et al. (2010). Comparative genomics reveals mobile pathogenicity chromosomes in Fusarium. Nature *464*, 367–373. https://doi.org/10.1038/nature08850.

5. Gibson, B., and Liti, G. (2015). Saccharomyces pastorianus: genomic insights inspiring innovation for industry. Yeast Chichester Engl. *32*, 17–27. https://doi.org/10.1002/yea.3033.

6. Mergoum, M., Singh, P.K., Peña, R.J., Lozano-del Río, A.J., Cooper, K.V., Salmon, D.F., and Gómez Macpherson, H. (2009). Triticale: A “New” Crop with Old Challenges. In Cereals, M. J. Carena, ed. (Springer US), pp. 267–287. https://doi.org/10.1007/978-0-387-72297-9_9.

7. Chen, Z.J. (2013). Genomic and epigenetic insights into the molecular bases of heterosis. Nat. Rev. Genet. *14*, 471–482. https://doi.org/10.1038/nrg3503.

8. Landry, C.R., Hartl, D.L., and Ranz, J.M. (2007). Genome clashes in hybrids: insights from gene expression. Heredity *99*, 483–493. https://doi.org/10.1038/sj.hdy.6801045.

9. Signor, S.A., and Nuzhdin, S.V. (2018). The Evolution of Gene Expression in cis and trans. Trends Genet. TIG *34*, 532–544. https://doi.org/10.1016/j.tig.2018.03.007.

10. Wittkopp, P.J., Haerum, B.K., and Clark, A.G. (2004). Evolutionary changes in cis and trans gene regulation. Nature *430*, 85–88. https://doi.org/10.1038/nature02698.

11. Tirosh, I., Reikhav, S., Levy, A.A., and Barkai, N. (2009). A Yeast Hybrid Provides Insight into the Evolution of Gene Expression Regulation. Science *324*, 659–662. https://doi.org/10.1126/science.1169766.

12. Bullard, J.H., Mostovoy, Y., Dudoit, S., and Brem, R.B. (2010). Polygenic and directional regulatory evolution across pathways in Saccharomyces. Proc. Natl. Acad. Sci. U. S. A. *107*, 5058–5063. https://doi.org/10.1073/pnas.0912959107.

13. Emerson, J.J., Hsieh, L.C., Sung, H.M., Wang, T.Y., Huang, C.J., Lu, H.H.S., Lu, M.Y.J., Wu, S.H., and Li, W.H. (2010). Natural selection on cis and trans regulation in yeasts. Genome Res. *20*, 826–836. https://doi.org/10.1101/gr.101576.109.

14. Fraser, H.B., Levy, S., Chavan, A., Shah, H.B., Perez, J.C., Zhou, Y., Siegal, M.L., and Sinha, H. (2012). Polygenic cis-regulatory adaptation in the evolution of yeast pathogenicity. Genome Res. *22*, 1930–1939. https://doi.org/10.1101/gr.134080.111.

15. Li, X.C., and Fay, J.C. (2017). Cis-regulatory divergence in gene expression between two thermally divergent yeast species. Genome Biol. Evol. *9*, 1120–1129. https://doi.org/10.1093/gbe/evx072.

16. Metzger, B.P.H., Wittkopp, P.J., and Coolon, J.D. (2017). Evolutionary Dynamics of Regulatory Changes Underlying Gene Expression Divergence among Saccharomyces Species. Genome Biol. Evol. *9*, 843–854. https://doi.org/10.1093/gbe/evx035.

17. Krieger, G., Lupo, O., Levy, A.A., and Barkai, N. (2020). Independent evolution of transcript abundance and gene regulatory dynamics. Genome Res. *30*, 1000–1011. https://doi.org/10.1101/gr.261537.120.

18. Gombert, A.K., Madeira, J.V., Cerdán, M.-E., and González-Siso, M.-I. (2016). Kluyveromyces marxianus as a host for heterologous protein synthesis. Appl. Microbiol. Biotechnol. *100*, 6193–6208. https://doi.org/10.1007/s00253-016-7645-y.

19. Bilal, M., Ji, L., Xu, Y., Xu, S., Lin, Y., Iqbal, H.M.N., and Cheng, H. (2022). Bioprospecting Kluyveromyces marxianus as a Robust Host for Industrial Biotechnology. Front. Bioeng. Biotechnol. *10*, 851768. https://doi.org/10.3389/fbioe.2022.851768.

20. Groeneveld, P., Stouthamer, A.H., and Westerhoff, H.V. (2009). Super life – how and why 'cell selection' leads to the fastest-growing eukaryote. FEBS J. *276*, 254–270. https://doi.org/10.1111/j.1742-4658.2008.06778.x.

21. Lertwattanasakul, N., Rodrussamee, N., Suprayogi, Limtong, S., Thanonkeo, P., Kosaka, T., and Yamada, M. (2011). Utilization capability of sucrose, raffinose and inulin and its less-sensitiveness to glucose repression in thermotolerant yeast Kluyveromyces marxianus DMKU 3-1042. AMB Express *1*, 20. https://doi.org/10.1186/2191-0855-1-20.

22. Rodrussamee, N., Lertwattanasakul, N., Hirata, K., Suprayogi, Limtong, S., Kosaka, T., and Yamada, M. (2011). Growth and ethanol fermentation ability on hexose and pentose sugars and glucose effect under various conditions in thermotolerant yeast Kluyveromyces marxianus. Appl. Microbiol. Biotechnol. *90*, 1573–1586. https://doi.org/10.1007/s00253-011-3218-2.

23. Fisk, D.G., Ball, C.A., Dolinski, K., Engel, S.R., Hong, E.L., Issel-Tarver, L., Schwartz, K., Sethuraman, A., Botstein, D., and Michael Cherry, J. (2006). Saccharomyces cerevisiae S288C genome annotation: a working hypothesis. Yeast *23*, 857–865. https://doi.org/10.1002/yea.1400.

24. Witte, V., Grossmann, B., and Emeis, C.C. (1989). Molecular probes for the detection of Kluyveromyces marxianus chromosomal DNA in electrophoretic karyotypes of intergeneric protoplast fusion products. Arch. Microbiol. *152*, 441–446. https://doi.org/10.1007/BF00446926.

25. Albonico, F., B, E., G, P.H., and B, D. (2022). New Saccharomyces cerevisiae-Kluyveromyces marxianus fusant shows enhanced alcoholic fermentation performance. World J. Microbiol. Biotechnol. *38*, 251. https://doi.org/10.1007/s11274-022-03422-1.

26. Fournier, R.E., and Ruddle, F.H. (1977). Microcell-mediated transfer of murine chromosomes into mouse, Chinese hamster, and human somatic cells. Proc. Natl. Acad. Sci. *74*, 319–323. https://doi.org/10.1073/pnas.74.1.319.

27. Fukagawa, T., Nogami, M., Yoshikawa, M., Ikeno, M., Okazaki, T., Takami, Y., Nakayama, T., and Oshimura, M. (2004). Dicer is essential for formation of the heterochromatin structure in vertebrate cells. Nat. Cell Biol. *6*, 784–791. https://doi.org/10.1038/ncb1155.

28. O'Doherty, A., Ruf, S., Mulligan, C., Hildreth, V., Errington, M.L., Cooke, S., Sesay, A., Modino, S., Vanes, L., Hernandez, D., et al. (2005). An aneuploid mouse strain carrying human chromosome 21 with Down syndrome phenotypes. Science *309*, 2033–2037. https://doi.org/10.1126/science.1114535.

29. Wilson, M.D., Barbosa-Morais, N.L., Schmidt, D., Conboy, C.M., Vanes, L., Tybulewicz, V.L.J., Fisher, E.M.C., Tavaré, S., and Odom, D.T. (2008). Species-specific transcription in mice carrying human chromosome 21. Science *322*, 434–438. https://doi.org/10.1126/science.1160930.

30. Lartigue, C., Glass, J.I., Alperovich, N., Pieper, R., Parmar, P.P., Hutchison, C.A., Smith, H.O., and Venter, J.C. (2007). Genome transplantation in bacteria: changing one species to another. Science *317*, 632–638. https://doi.org/10.1126/science.1144622.

31. Shen, X.-X., Opulente, D.A., Kominek, J., Zhou, X., Steenwyk, J.L., Buh, K.V., Haase, M.A.B., Wisecaver, J.H., Wang, M., Doering, D.T., et al. (2018). Tempo and Mode of Genome Evolution in the Budding Yeast Subphylum. Cell *175*, 1533-1545.e20. https://doi.org/10.1016/j.cell.2018.10.023.

32. Kitaoka, M., Smith, O.K., Straight, A.F., and Heald, R. (2022). Molecular conflicts disrupting centromere maintenance contribute to Xenopus hybrid inviability. Curr. Biol. CB *32*, 3939-3951.e6. https://doi.org/10.1016/j.cub.2022.07.037.

33. Kitano, J., and Okude, G. (2024). Causative genes of intrinsic hybrid incompatibility in animals and plants: what we have learned about speciation from the molecular perspective. Evol. J. Linn. Soc. *3*, kzae022. https://doi.org/10.1093/evolinnean/kzae022.

34. Lartigue, C., Vashee, S., Algire, M.A., Chuang, R.-Y., Benders, G.A., Ma, L., Noskov, V.N., Denisova, E.A., Gibson, D.G., Assad-Garcia, N., et al. (2009). Creating bacterial strains from genomes that have been cloned and engineered in yeast. Science *325*, 1693–1696. https://doi.org/10.1126/science.1173759.

35. Minh, B.Q., Schmidt, H.A., Chernomor, O., Schrempf, D., Woodhams, M.D., von Haeseler, A., and Lanfear, R. (2020). IQ-TREE 2: New Models and Efficient Methods for Phylogenetic Inference in the Genomic Era. Mol. Biol. Evol. *37*, 1530–1534. https://doi.org/10.1093/molbev/msaa015.

36. Emms, D.M., and Kelly, S. (2019). OrthoFinder: phylogenetic orthology inference for comparative genomics. Genome Biol. *20*, 238. https://doi.org/10.1186/s13059-019-1832-y.

37. Peska, V., Fajkus, P., Bubeník, M., Brázda, V., Bohálová, N., Dvořáček, V., Fajkus, J., and Garcia, S. (2021). Extraordinary diversity of telomeres, telomerase RNAs and their template regions in Saccharomycetaceae. Sci. Rep. *11*, 12784. https://doi.org/10.1038/s41598-021-92126-x.

38. Shao, Y., Lu, N., Wu, Z., Cai, C., Wang, S., Zhang, L.-L., Zhou, F., Xiao, S., Liu, L., Zeng, X., et al. (2018). Creating a functional single-chromosome yeast. Nature *560*, 331–335. https://doi.org/10.1038/s41586-018-0382-x.

39. Nieduszynski, C.A., Knox, Y., and Donaldson, A.D. (2006). Genome-wide identification of replication origins in yeast by comparative genomics. Genes Dev. *20*, 1874–1879. https://doi.org/10.1101/gad.385306.

40. Noskov, V.N., Chuang, R.-Y., Gibson, D.G., Leem, S.-H., Larionov, V., and Kouprina, N. (2011). Isolation of circular yeast artificial chromosomes for synthetic biology and functional genomics studies. Nat. Protoc. *6*, 89–96. https://doi.org/10.1038/nprot.2010.174.

41. Lyu, Y., Wu, P., Zhou, J., Yu, Y., and Lu, H. (2021). Protoplast transformation of Kluyveromyces marxianus. Biotechnol. J. *16*, e2100122. https://doi.org/10.1002/biot.202100122.

42. Tschumper, G., and Carbon, J. (1986). High frequency excision of Ty elements during transformation of yeast. Nucleic Acids Res. *14*, 2989–3001. https://doi.org/10.1093/nar/14.7.2989.

43. Wu, P., Mo, W., Tian, T., Song, K., Lyu, Y., Ren, H., Zhou, J., Yu, Y., and Lu, H. (2024). Transfer of disulfide bond formation modules via yeast artificial chromosomes promotes the expression of heterologous proteins in Kluyveromyces marxianus. mLife *3*, 129–142. https://doi.org/10.1002/mlf2.12115.

44. Travesa, A., and Wittenberg, C. (2012). Turned on by genotoxic stress. Cell Cycle Georget. Tex *11*, 3145–3146. https://doi.org/10.4161/cc.21587.

45. Walker, G.M., and Basso, T.O. (2020). Mitigating stress in industrial yeasts. Fungal Biol. *124*, 387–397. https://doi.org/10.1016/j.funbio.2019.10.010.

46. Coluccio, A., Bogengruber, E., Conrad, M.N., Dresser, M.E., Briza, P., and Neiman, A.M. (2004). Morphogenetic pathway of spore wall assembly in Saccharomyces cerevisiae. Eukaryot. Cell *3*, 1464–1475. https://doi.org/10.1128/EC.3.6.1464-1475.2004.

47. Chakrabortee, S., Byers, J.S., Jones, S., Garcia, D.M., Bhullar, B., Chang, A., She, R., Lee, L., Fremin, B., Lindquist, S., et al. (2016). Intrinsically Disordered Proteins Drive Emergence and Inheritance of Biological Traits. Cell *167*, 369-381.e12. https://doi.org/10.1016/j.cell.2016.09.017.

48. Soares, E.V. (2011). Flocculation in Saccharomyces cerevisiae: a review. J. Appl. Microbiol. *110*, 1–18. https://doi.org/10.1111/j.1365-2672.2010.04897.x.

49. Teunissen, A.W., and Steensma, H.Y. (1995). Review: the dominant flocculation genes of Saccharomyces cerevisiae constitute a new subtelomeric gene family. Yeast Chichester Engl. *11*, 1001–1013. https://doi.org/10.1002/yea.320111102.

50. Brothers, M., and Rine, J. (2022). Distinguishing between recruitment and spread of silent chromatin structures in Saccharomyces cerevisiae. eLife *11*, e75653. https://doi.org/10.7554/eLife.75653.

51. Sjöstrand, J.O.O., Kegel, A., and Aström, S.U. (2002). Functional diversity of silencers in budding yeasts. Eukaryot. Cell *1*, 548–557. https://doi.org/10.1128/EC.1.4.548-557.2002.

52. Aström, S.U., Kegel, A., Sjöstrand, J.O., and Rine, J. (2000). Kluyveromyces lactis Sir2p regulates cation sensitivity and maintains a specialized chromatin structure at the cryptic alpha-locus. Genetics *156*, 81–91. https://doi.org/10.1093/genetics/156.1.81.

53. De Boer, C.G., and Hughes, T.R. (2012). YeTFaSCo: A database of evaluated yeast transcription factor sequence specificities. Nucleic Acids Res. *40*, 169–179. https://doi.org/10.1093/nar/gkr993.

54. Lai, H.-Y., Yu, Y.-H., Jhou, Y.-T., Liao, C.-W., and Leu, J.-Y. (2023). Multiple intermolecular interactions facilitate rapid evolution of essential genes. Nat. Ecol. Evol. *7*, 745–755. https://doi.org/10.1038/s41559-023-02029-5.

55. Byrne, K.P., and Wolfe, K.H. (2005). The Yeast Gene Order Browser: combining curated homology and syntenic context reveals gene fate in polyploid species. Genome Res. *15*, 1456–1461. https://doi.org/10.1101/gr.3672305.

56. Gabaldón, T., and Koonin, E.V. (2013). Functional and evolutionary implications of gene orthology. Nat. Rev. Genet. *14*, 360–366. https://doi.org/10.1038/nrg3456.

57. Pobiega, S., and Marcand, S. (2010). Dicentric breakage at telomere fusions. Genes Dev. *24*, 720–733. https://doi.org/10.1101/gad.571510.

58. Postma, E.D., Dashko, S., van Breemen, L., Taylor Parkins, S.K., van den Broek, M., Daran, J.-M., and Daran-Lapujade, P. (2021). A supernumerary designer chromosome for modular in vivo pathway assembly in Saccharomyces cerevisiae. Nucleic Acids Res. *49*, 1769–1783. https://doi.org/10.1093/nar/gkaa1167.

59. Zhou, J., Zhang, C., Wei, R., Han, M., Wang, S., Yang, K., Zhang, L., Chen, W., Wen, M., Li, C., et al. (2022). Exogenous artificial DNA forms chromatin structure with active transcription in yeast. Sci. China Life Sci. *65*, 851–860. https://doi.org/10.1007/s11427-021-2044-x.

60. Gibson, D.G., Glass, J.I., Lartigue, C., Noskov, V.N., Chuang, R.-Y., Algire, M.A., Benders, G.A., Montague, M.G., Ma, L., Moodie, M.M., et al. (2010). Creation of a bacterial cell controlled by a chemically synthesized genome. Science *329*, 52–56. https://doi.org/10.1126/science.1190719.

61. Peris, D., Alexander, W.G., Fisher, K.J., Moriarty, R.V., Basuino, M.G., Ubbelohde, E.J., Wrobel, R.L., and Hittinger, C.T. (2020). Synthetic hybrids of six yeast species. Nat. Commun. *11*, 2085. https://doi.org/10.1038/s41467-020-15559-4.

62. Nonklang, S., Ano, A., Abdel-Banat, B.M.A., Saito, Y., Hoshida, H., and Akada, R. (2009). Construction of flocculent Kluyveromyces marxianus strains suitable for high-temperature ethanol fermentation. Biosci. Biotechnol. Biochem. *73*, 1090–1095. https://doi.org/10.1271/bbb.80853.

63. Sasanuma, H., Hirota, K., Fukuda, T., Kakusho, N., Kugou, K., Kawasaki, Y., Shibata, T., Masai, H., and Ohta, K. (2008). Cdc7-dependent phosphorylation of Mer2 facilitates initiation of yeast meiotic recombination. Genes Dev. *22*, 398–410. https://doi.org/10.1101/gad.1626608.

64. Nguyen, T.H., Fleet, G.H., and Rogers, P.L. (1998). Composition of the cell walls of several yeast species. Appl. Microbiol. Biotechnol. *50*, 206–212. https://doi.org/10.1007/s002530051278.

65. Fredens, J., Wang, K., de la Torre, D., Funke, L.F.H., Robertson, W.E., Christova, Y., Chia, T., Schmied, W.H., Dunkelmann, D.L., Beránek, V., et al. (2019). Total synthesis of Escherichia coli with a recoded genome. Nature *569*, 514–518. https://doi.org/10.1038/s41586-019-1192-5.

66. Venetz, J.E., Del Medico, L., Wölfle, A., Schächle, P., Bucher, Y., Appert, D., Tschan, F., Flores-Tinoco, C.E., van Kooten, M., Guennoun, R., et al. (2019). Chemical synthesis rewriting of a bacterial genome to achieve design flexibility and biological functionality. Proc. Natl. Acad. Sci. U. S. A. *116*, 8070–8079. https://doi.org/10.1073/pnas.1818259116.

67. Meiklejohn, C.D., Coolon, J.D., Hartl, D.L., and Wittkopp, P.J. (2014). The roles of cis- and trans-regulation in the evolution of regulatory incompatibilities and sexually dimorphic gene expression. Genome Res. *24*, 84–95. https://doi.org/10.1101/gr.156414.113.

68. Guerrero, R.F., Posto, A.L., Moyle, L.C., and Hahn, M.W. (2016). Genome-wide patterns of regulatory divergence revealed by introgression lines. Evol. Int. J. Org. Evol. *70*, 696–706. https://doi.org/10.1111/evo.12875.

69. Gordon, K.L., and Ruvinsky, I. (2012). Tempo and Mode in Evolution of Transcriptional Regulation. PLoS Genet. *8*, e1002432. https://doi.org/10.1371/journal.pgen.1002432.

70. Zhou, J., Zhu, P., Hu, X., Lu, H., and Yu, Y. (2018). Improved secretory expression of lignocellulolytic enzymes in Kluyveromyces marxianus by promoter and signal sequence engineering. Biotechnol. Biofuels *11*, 235. https://doi.org/10.1186/s13068-018-1232-7.

71. Amberg, D.C., Burke, D., Strathern, J.N., and Burke, D. (2005). Methods in yeast genetics: a Cold Spring Harbor Laboratory course manual 2005 ed. (Cold Spring Harbor Laboratory Press).

72. Ren, H., Yin, A., Wu, P., Zhou, H., Zhou, J., Yu, Y., and Lu, H. (2022). Establishment of a Cre-loxP System Based on a Leaky LAC4 Promoter and an Unstable panARS Element in Kluyveromyces marxianus. Microorganisms *10*, 1240. https://doi.org/10.3390/microorganisms10061240.

73. Antunes, D.F., de Souza Junior, C.G., and de Morais Junior, M.A. (2000). A simple and rapid method for lithium acetate-mediated transformation of Kluyveromyces marxianus cells. World J. Microbiol. Biotechnol. *16*, 653–654. https://doi.org/10.1023/A:1008984403732.

74. Gietz, R.D., and Schiestl, R.H. (2007). Large-scale high-efficiency yeast transformation using the LiAc/SS carrier DNA/PEG method. Nat. Protoc. *2*, 38–41. https://doi.org/10.1038/nprot.2007.16.

75. Shi, T., Zeng, J., Zhou, J., Yu, Y., and Lu, H. (2022). Correlation Between Improved Mating Efficiency and Weakened Scaffold-Kinase Interaction in the Mating Pheromone Response Pathway Revealed by Interspecies Complementation. Front. Microbiol. *13*, 865829. https://doi.org/10.3389/fmicb.2022.865829.

76. Shao, Y., Lu, N., Qin, Z., and Xue, X. (2018). CRISPR-Cas9 Facilitated Multiple-Chromosome Fusion in Saccharomyces cerevisiae. ACS Synth. Biol. *7*, 2706–2708. https://doi.org/10.1021/acssynbio.8b00397.

77. Li, H., and Durbin, R. (2009). Fast and accurate short read alignment with Burrows-Wheeler transform. Bioinforma. Oxf. Engl. *25*, 1754–1760. https://doi.org/10.1093/bioinformatics/btp324.

78. McKenna, A., Hanna, M., Banks, E., Sivachenko, A., Cibulskis, K., Kernytsky, A., Garimella, K., Altshuler, D., Gabriel, S., Daly, M., et al. (2010). The Genome Analysis Toolkit: a MapReduce framework for analyzing next-generation DNA sequencing data. Genome Res. *20*, 1297–1303. https://doi.org/10.1101/gr.107524.110.

79. Yu, Y., Mo, W., Ren, H., Yang, X., Lu, W., Luo, T., Zeng, J., Zhou, J., Qi, J., and Lu, H. (2021). Comparative Genomic and Transcriptomic Analysis Reveals Specific Features of Gene Regulation in Kluyveromyces marxianus. Front. Microbiol. *12*, 598060. https://doi.org/10.3389/fmicb.2021.598060.

80. Danecek, P., Auton, A., Abecasis, G., Albers, C.A., Banks, E., DePristo, M.A., Handsaker, R.E., Lunter, G., Marth, G.T., Sherry, S.T., et al. (2011). The variant call format and VCFtools. Bioinformatics *27*, 2156–2158. https://doi.org/10.1093/bioinformatics/btr330.

81. Matheson, K., Parsons, L., and Gammie, A. (2017). Whole-Genome Sequence and Variant Analysis of W303, a Widely-Used Strain of Saccharomyces cerevisiae. G3 Bethesda Md *7*, 2219–2226. https://doi.org/10.1534/g3.117.040022.

82. Miao, Z., Ren, Y., Tarabini, A., Yang, L., Li, H., Ye, C., Liti, G., Fischer, G., Li, J., and Yue, J.-X. (2025). ScRAPdb: an integrated pan-omics database for the Saccharomyces cerevisiae reference assembly panel. Nucleic Acids Res. *53*, D852–D863. https://doi.org/10.1093/nar/gkae955.

83. Danecek, P., Bonfield, J.K., Liddle, J., Marshall, J., Ohan, V., Pollard, M.O., Whitwham, A., Keane, T., McCarthy, S.A., Davies, R.M., et al. (2021). Twelve years of SAMtools and BCFtools. GigaScience *10*, giab008. https://doi.org/10.1093/gigascience/giab008.

84. Anders, S., Pyl, P.T., and Huber, W. (2015). HTSeq--a Python framework to work with high-throughput sequencing data. Bioinformatics *31*, 166–169. https://doi.org/10.1093/bioinformatics/btu638.

85. Love, M.I., Huber, W., and Anders, S. (2014). Moderated estimation of fold change and dispersion for RNA-seq data with DESeq2. Genome Biol. *15*, 550. https://doi.org/10.1186/s13059-014-0550-8.

86. Stephens, M. (2017). False discovery rates: a new deal. Biostat. Oxf. Engl. *18*, 275–294. https://doi.org/10.1093/biostatistics/kxw041.

87. Fraser, H.B. (2019). Improving Estimates of Compensatory cis-trans Regulatory Divergence. Trends Genet. TIG *35*, 3–5. https://doi.org/10.1016/j.tig.2018.09.003.

88. Wagih, O., and Parts, L. (2014). gitter: a robust and accurate method for quantification of colony sizes from plate images. G3 Bethesda Md *4*, 547–552. https://doi.org/10.1534/g3.113.009431.

Acknowledgments

Funding:

Science and Technology Research Program of Shanghai 24ZR1406500 (YY)

National Key Research and Development Program of China grant 2021YFA0910603 (YY)

National Key Research and Development Program of China grant 2022YFC2106201 (JZ)

National Key Research and Development Program of China grant 2021YFA0910601 (HL)

Science and Technology Research Program of Shanghai grant 2023ZX01 (HL)

Open Fund of State Key Laboratory of Genetic Engineering grant SKLGE-2318 (YY)

The Fundamental Research Funds for the Central Universities (XCL)

Young Scientists Fund of the National Natural Science Foundation of China, grant #32400495 (XCL).

Author contributions:

Conceptualization: HL, YY

Methodology: HL, YY, YL

Investigation: YL, KS, JZ, HC, XCL

Writing—original draft: YL, YY

Writing—review & editing: YL, YY, YW, XH, XCL

Competing interests:

Authors declare that they have no competing interests.

Data and materials availability:

DNA-seq and RNA-seq data are available in the NCBI.

(https://dataview.ncbi.nlm.nih.gov/object/PRJNA1102743?reviewer=98okerqm686mrj3ddq79r4l18u)

Supplementary Materials

Fig. S1. Transformation efficiency and stability of plasmids containing different combinations of *ARS* and *CEN* from Km and Sc.

Fig. S2. Zygotes formed between Km cells and between Sc cells.

Fig. S3. Growth of Sc-R1 and Sc-R3.

Fig. S4. Identification of a 29 kb deletion in R3.

Fig. S5. PFGE of Km chromosomes.

Fig. S6. Growth of hybrids and their parental strains under various conditions.

Fig. S7. Growth of KS-R1 and KS-R3 after loss of Sc chromosomes.

Fig. S8. Flocculation of Km and KS-R1ΔR1.

Fig. S9. Expression differences along R1 and R3 chromosomes under YPD, TM and NaCl conditions.

Fig. S10. PCA of gene expression under NaCl and TM conditions.

Fig. S11. Divergence of orthologous genes.

Supplementary Data File 1. Donors used in the engineering of Sc chr1 and chr3.

Supplementary Data File 2. Raw read counts of RNA-seq data and batch information.

Table S1. Primers used in this study, along with manually curated R1 and R3 sequences.

Table S2. SNPs and INDELs on Km chromosomes of KS-R1 & KS-R3.

Table S3. Differential expression of Sc and Km genes upon chromosomal transfers.

Table S4. Orthologous genes in Km and Sc (W303).

Table S5. *Cis*, *trans* and *cis+trans* effects based on allele-specific expression.

Table S6. Expression changes in Sc-specific genes vs. orthologous genes.

Table S7. Strains used in this study.

Table S8. Plasmids used in this study, and sequences of LHZ626, LHZ1495 and pRS425-Cas9-2xSapI.

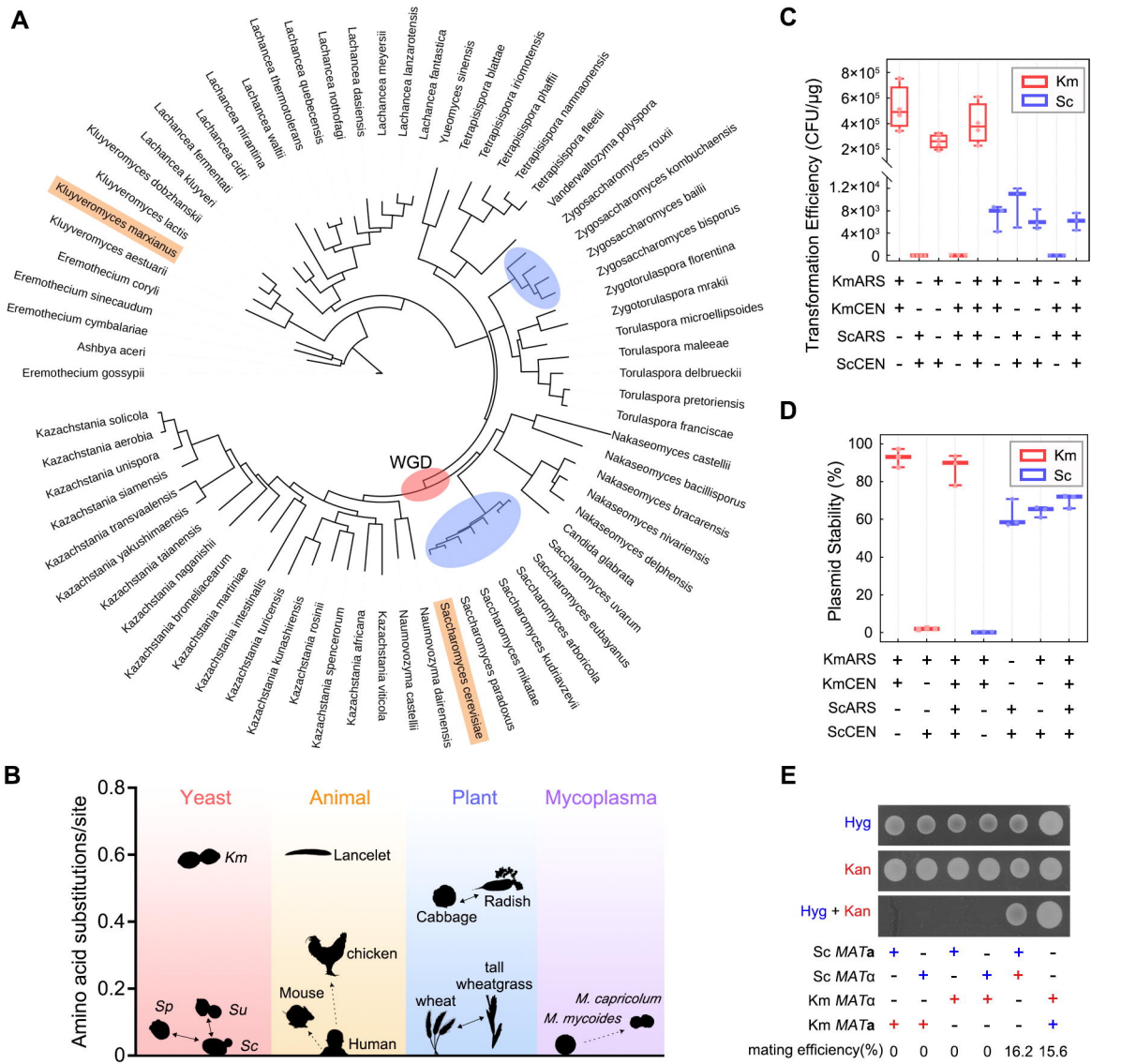
A
Lachancea thermotolerans
Lachancea quebecensis
Lachancea nothofagi
Lachancea dasiensis
Lachancea meyersii
Lachancea lanzarotensis
Lachancea fantastica
Yueomyces sinensis
Tetrapisispora blattae
Tetrapisispora iriomotensis
Tetrapisispora phaffii
Tetrapisispora namnaonensis
Tetrapisispora fleetii
Vanderwaltozyma polyspora
Zygosaccharomyces rouxii
Zygosaccharomyces kombuchaensis
Zygosaccharomyces bailii
Zygosaccharomyces bisporus
Zygotorulaspora florentina
Zygotorulaspora mrakii
Torulaspora microellipsoides
Torulaspora maleeae
Torulaspora delbrueckii
Torulaspora pretoriensis
Torulaspora franciscae
Nakaseomyces castellii
Nakaseomyces bacillisporus
Nakaseomyces bracarensis
Nakaseomyces nivariensis
Nakaseomyces delphensis
Candida glabrata
Saccharomyces uvarum
Saccharomyces eubayanus
Saccharomyces arboricola
Saccharomyces kudriavzevii
Saccharomyces mikatae
Saccharomyces paradoxus
Saccharomyces cerevisiae
Naumovozyma dairenensis
Naumovozyma castellii
Kazachstania viticola
Kazachstania africana
Kazachstania spencerorum
Kazachstania rosinii
Kazachstania kunashirensis
Kazachstania turicensis
Kazachstania intestinalis
Kazachstania martiniae
Kazachstania bromeliacearum
Kazachstania naganishii
Kazachstania talanensis
Kazachstania yakushimaensis
Kazachstania transvaalensis
Kazachstania siamensis
Kazachstania unispora
Kazachstania aerobia
Kazachstania solicola
Lachancea mirantina
Lachancea cidri
Lachancea fermentati
Lachancea kluyveri
Kluyveromyces dobzhanskii
Kluyveromyces lactis
Kluyveromyces marxianus
Kluyveromyces aestuarii
Eremothecium coryli
Eremothecium sinecaudum
Eremothecium cymbalariae
Ashbya aceri
Eremothecium gossypii
Lachancea wallii
WGD
C
Transformation Efficiency (CFU/μg)
8×10^5
6×10^5
4×10^5
2×10^5
1.2×10^4
8×10^3
4×10^3
0
Km
Sc
KmARS + - + - + + - + - +
KmCEN + - - + + + - - + +
ScARS - + - + + - + - + +
ScCEN - + + - + + + + - +
D
Plasmid Stability (%)
100
80
60
40
20
0
Km
Sc
KmARS + + + + - + +
KmCEN + - + + - - +
ScARS - - + - + - +
ScCEN - + + - + + +
B
Amino acid substitutions/site
0.8
0.6
0.4
0.2
0
Yeast
Animal
Plant
Mycoplasma
Km
Sp
Su
Sc
Lancelet
chicken
Mouse
Human
Radish
Cabbage
tall wheatgrass
wheat
M. capricolum
M. mycoides
E
Hyg
Kan
Hyg + Kan
Sc MATa + - + - + -
Sc MATα - + - + + -
Km MATα - - + + - +
Km MATa + + - - - +
mating efficiency(%) 0 0 0 0 16.2 15.6

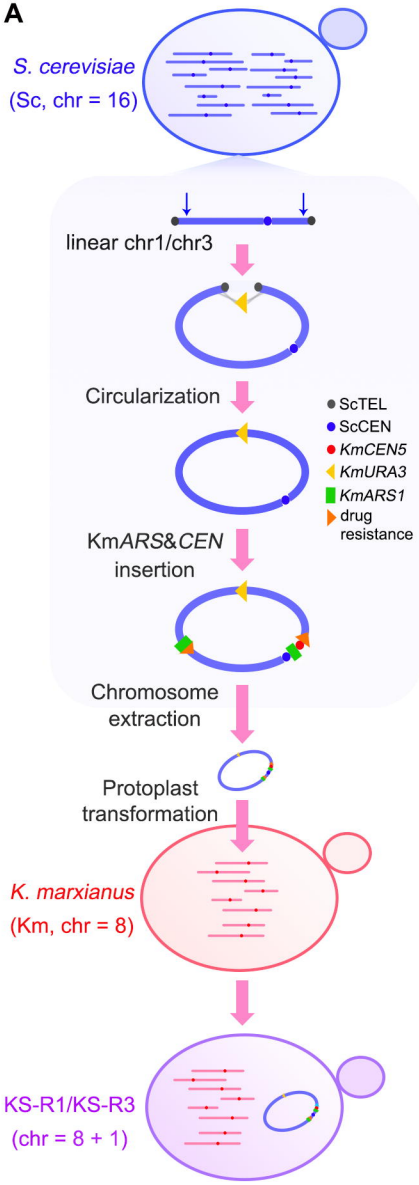

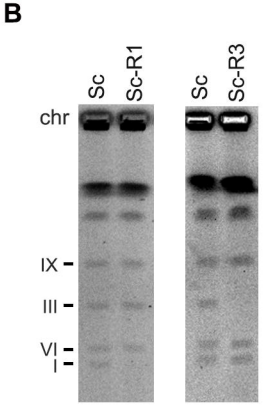

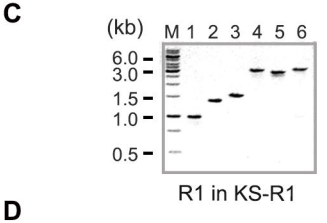

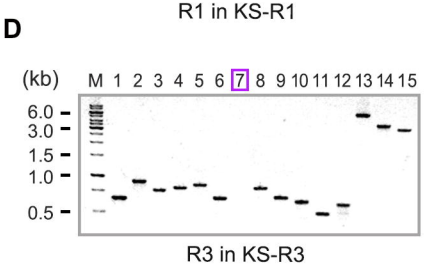

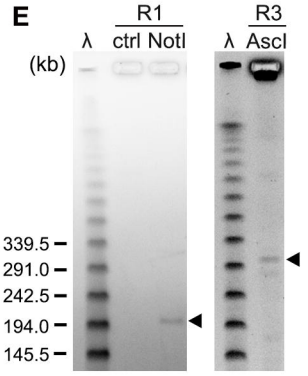

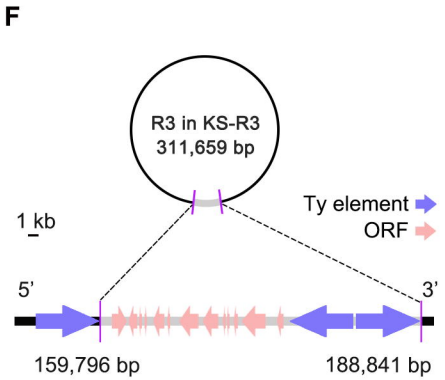

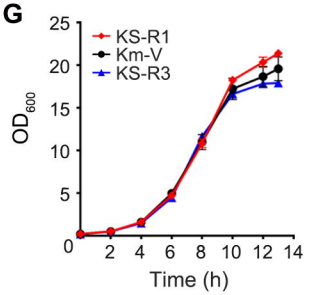

H

Strain	Circular chromosome	Loss frequency per generation (%)
KS-R1	R1	0.11
KS-R3	R3	0.84

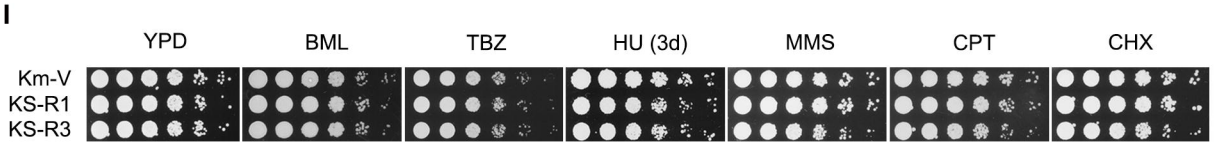

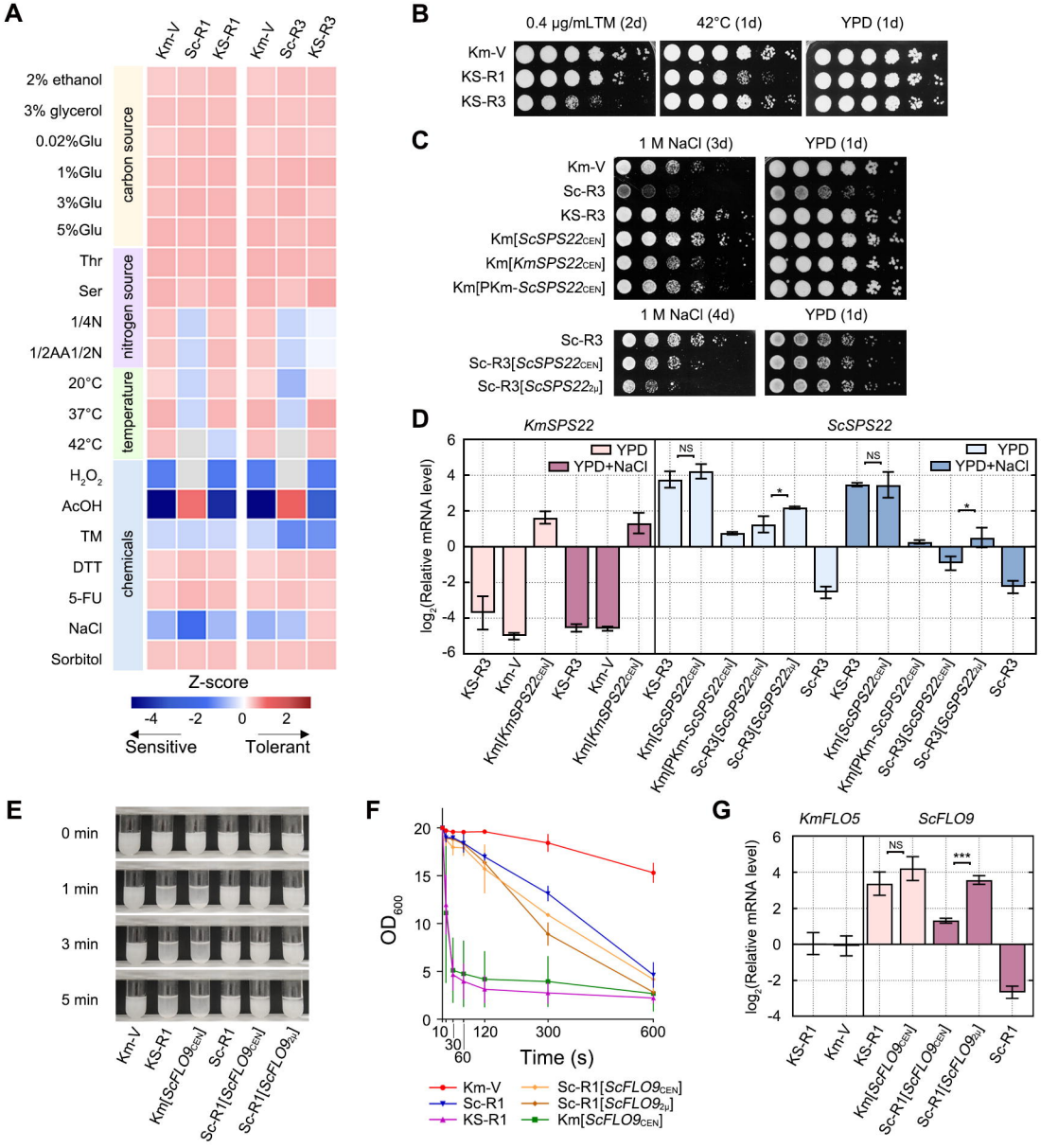
A
Km-V
Sc-R1
KS-R1
Km-V
Sc-R3
KS-R3
2% ethanol
3% glycerol
0.02%Glu
1%Glu
3%Glu
5%Glu
carbon source
Thr
Ser
1/4N
1/2AA1/2N
nitrogen source
20°C
37°C
42°C
temperature
H2O2
AcOH
TM
DTT
5-FU
NaCl
Sorbitol
chemicals
Z-score
-4
-2
0
2
Sensitive
Tolerant
B
0.4 μg/mLTM (2d)
42°C (1d)
YPD (1d)
Km-V
KS-R1
KS-R3
C
1 M NaCl (3d)
YPD (1d)
Km-V
Sc-R3
KS-R3
Km[ScSPS22CEN]
Km[KmSPS22CEN]
Km[PKm-ScSPS22CEN]
1 M NaCl (4d)
YPD (1d)
Sc-R3
Sc-R3[ScSPS22CEN]
Sc-R3[ScSPS22 2μ]
D
KmSPS22
ScSPS22
YPD
YPD+NaCl
NS
*
log2(Relative mRNA level)
6
4
2
0
-2
-4
-6
KS-R3
Km-V
Km[KmSPS22CEN]
KS-R3
Km-V
Km[KmSPS22CEN]
KS-R3
Km[ScSPS22CEN]
Km[PKm-ScSPS22CEN]
Sc-R3[ScSPS22CEN]
Sc-R3[ScSPS22 2μ]
Sc-R3
KS-R3
Km[ScSPS22CEN]
Km[PKm-ScSPS22CEN]
Sc-R3[ScSPS22CEN]
Sc-R3[ScSPS22 2μ]
Sc-R3
E
0 min
1 min
3 min
5 min
Km-V
KS-R1
Km[ScFLO9CEN]
Sc-R1
Sc-R1[ScFLO9CEN]
Sc-R1[ScFLO9 2μ]
F
OD600
20
15
10
5
0
10
30
60
120
300
600
Time (s)
Km-V
Sc-R1
KS-R1
Sc-R1[ScFLO9CEN]
Sc-R1[ScFLO9 2μ]
Km[ScFLO9CEN]
G
KmFLO5
ScFLO9
NS
***
log2(Relative mRNA level)
6
4
2
0
-2
-4
KS-R1
Km-V
KS-R1
Km[ScFLO9CEN]
Sc-R1[ScFLO9CEN]
Sc-R1[ScFLO9 2μ]
Sc-R1

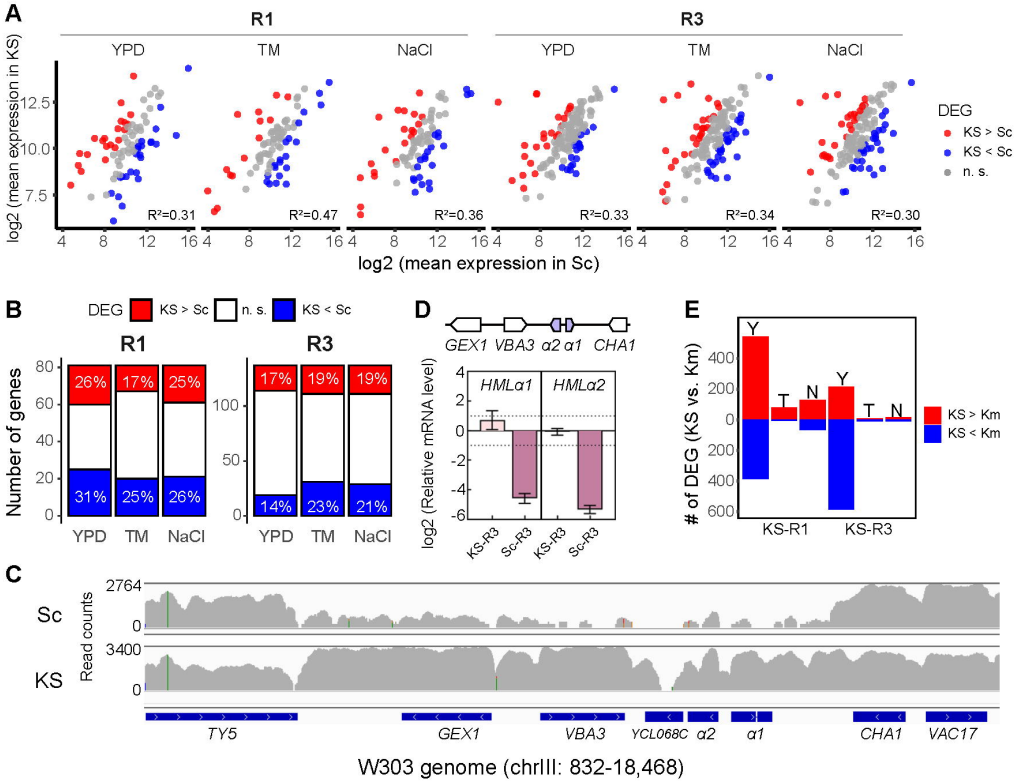
A
R1
R3
YPD
TM
NaCl
log2 (mean expression in KS)
log2 (mean expression in Sc)
R²=0.31
R²=0.47
R²=0.36
R²=0.33
R²=0.34
R²=0.30
DEG
KS > Sc
KS < Sc
n. s.
B
DEG
KS > Sc
n. s.
KS < Sc
Number of genes
26%
17%
25%
31%
25%
26%
17%
19%
19%
14%
23%
21%
D
GEX1 VBA3 α2 α1 CHA1
HMLα1
HMLα2
log2 (Relative mRNA level)
KS-R3
Sc-R3
E
# of DEG (KS vs. Km)
KS-R1
KS-R3
KS > Km
KS < Km
C
Sc
KS
Read counts
2764
3400
TY5
GEX1
VBA3
YCL068C
α2
α1
CHA1
VAC17
W303 genome (chrIII: 832-18,468)

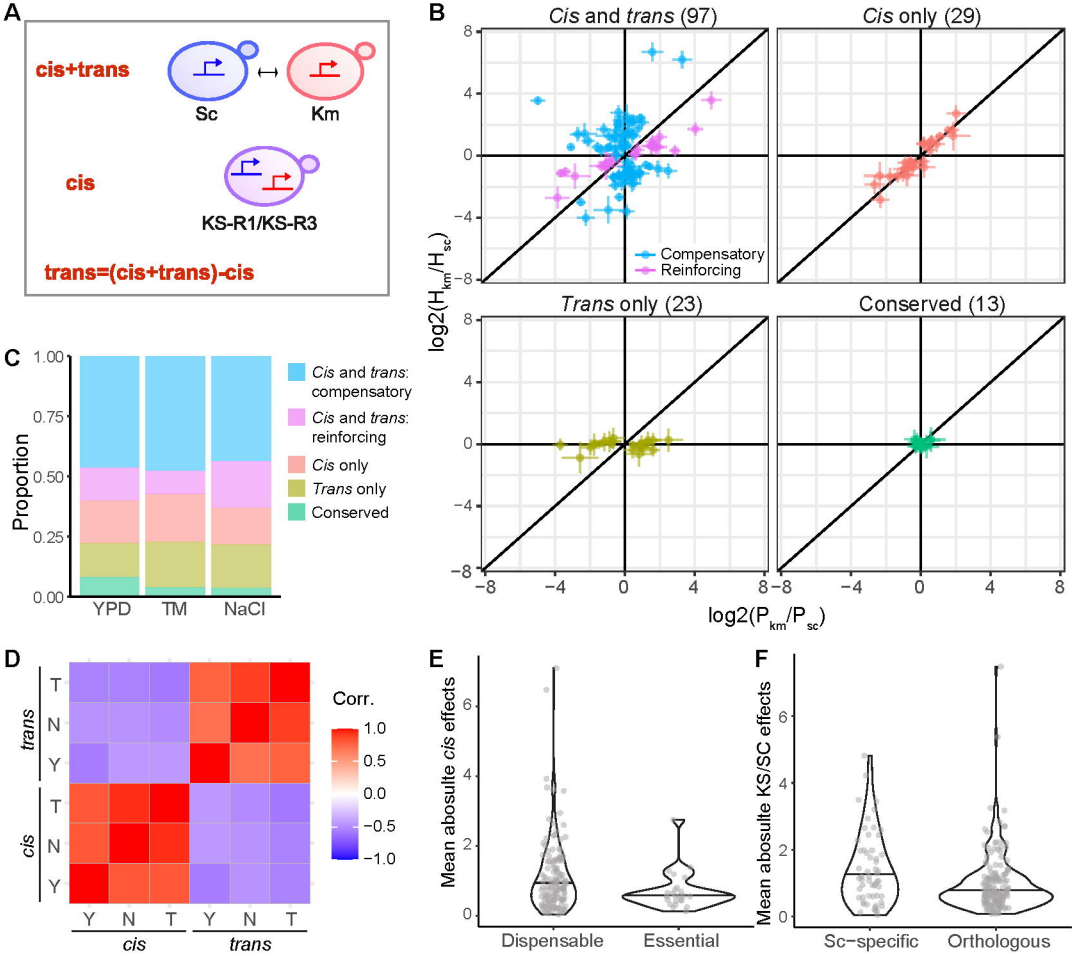
A
cis+trans
Sc
Km
cis
KS-R1/KS-R3
trans=(cis+trans)-cis
B
Cis and trans (97)
Cis only (29)
Trans only (23)
Conserved (13)
Compensatory
Reinforcing
log2(Hkm/Hsc)
log2(Pkm/Psc)
C
Proportion
Cis and trans: compensatory
Cis and trans: reinforcing
Cis only
Trans only
Conserved
YPD
TM
NaCl
D
trans
cis
Corr.
E
Mean abosulte cis effects
Dispensable
Essential
F
Mean abosulte KS/SC effects
Sc−specific
Orthologous